

5-2015

# Distinguishing Macrophage Activation States by Mass Spectrometry

Matthias Manfred Knust  
*University of Arkansas, Fayetteville*

Follow this and additional works at: <http://scholarworks.uark.edu/etd>

 Part of the [Analytical Chemistry Commons](#), and the [Biochemistry Commons](#)

---

## Recommended Citation

Knust, Matthias Manfred, "Distinguishing Macrophage Activation States by Mass Spectrometry" (2015). *Theses and Dissertations*. 7.  
<http://scholarworks.uark.edu/etd/7>

This Thesis is brought to you for free and open access by ScholarWorks@UARK. It has been accepted for inclusion in Theses and Dissertations by an authorized administrator of ScholarWorks@UARK. For more information, please contact [scholar@uark.edu](mailto:scholar@uark.edu), [ccmiddle@uark.edu](mailto:ccmiddle@uark.edu).

## Distinguishing Macrophage Activation States by Mass Spectrometry

# Distinguishing Macrophage Activation States by Mass Spectrometry

A thesis submitted in partial fulfillment  
of the requirements for the degree of  
Master of Science in Chemistry

by

Matthias Knust  
University of Regensburg  
Bachelor of Science in Chemistry, 2009  
University of Arkansas  
Bachelor of Science in Chemistry, 2009

May 2015  
University of Arkansas

This thesis is approved for recommendation to the Graduate Council.

---

Dr. Julie A. Stenken  
Thesis Director

---

Dr. Jackson O. Lay  
Committee Member

---

Dr. David W. Paul  
Committee Member

---

Dr. Suresh Kumar Thallapuranam  
Committee Member

## Abstract

Macrophages are versatile and highly adaptive cells that are involved in a wide range of physiological processes including host defense, homeostasis or regeneration, as well as pathogenesis. They react to their microenvironment, assuming various roles based on chemical and/or physical cues, and can reversibly shift between these so-called activation states. Concurrently, the technique of immunohistochemistry is used to gain spatial information on activated macrophages on tissue sections. The aim of this work was to find mass spectral biomarkers that allow the differentiation of activation states, and establish conditions that can be used in imaging mass spectrometry (IMS) experiments to investigate the spatial distribution of differently-activated macrophages within tissue sections. The immortalized macrophage line NR8383 (alveolar, rat) was used, and *in vitro* activated with the endotoxin lipopolysaccharide (LPS), or with the cytokine interleukin-4 (IL-4). In IMS, tissue sections are commonly prepared to be compatible with matrix assisted laser desorption/ionization (MALDI) mass spectrometry (MS) experiments. The tested combinations of MALDI preparation techniques and instrument parameters however remained unsuccessful at distinguishing activation states. Through lowering the complexity of the sample with a 30 minute high-performance liquid chromatography (HPLC) separation, a reproducible biomarker for LPS-activation could be found in electrospray ionization (ESI) MS experiments. The isolated biomarker was subjected to a tryptic digestion, and the resulting tryptic fragments analyzed by MALDI MS. A MASCOT database search suggested the macrophage-capping protein (CAPG) as source of the peptide, which could be validated through peptide sequencing through post-source decay experiments conducted on the tryptic fragments.

## **Acknowledgements**

I would like to express my sincere gratitude to my advisor, Dr. Julie A. Stenken, for all the time and effort she invested into me over the years. In uncertain times, she readily welcomed me into her group, and gave me the freedom and support to explore new techniques and to investigate fundamental relationships that helped me become a better scientist.

I would like to thank my research committee members, Dr. Jackson O. Lay, Dr. Suresh Kumar Thallapuram, and Dr. David W. Paul, for sharing their critical insights with me, and for reminding me of the many facets that one has to consider and re-visit in a research project. Additionally, I would like to express my sincere thanks to Dr. Lay for granting me access to use the instruments of the MS facility, and to the Koeppel group for letting me use their lyophilization set up.

I am grateful to Dr. Rohana Liyanage for training me on the mass spectrometers, for all his time and effort that went into trouble shooting the instruments, and for assisting me in gathering data on instruments that I could not operate by myself.

Special thanks to Jerry Homesley, Dave Parette, Shawn Fields, and KZ Shein from our technical support for all their help in trouble shooting the instruments, and for sharing their experience with instrumentation and electronics with me. To this end, I would also like to thank Dr. Bill Durham for letting my colleagues and I talk him into teaching us his workshop class.

Last but not least, I would like to express my deepest gratitude to my family and friends for supporting me through all the difficult decisions that came with graduate school, and for helping me retain sanity when I could not see the light at the end of the tunnel.

## Table of contents

Abstract .....	
Acknowledgements .....	
Table of contents .....	
List of Figures .....	
Glossary .....	
Chapter 1: Background and Significance .....	1
1.1. The Macrophage .....	1
1.1.1. A cell type with many functions .....	1
1.1.2. Macrophage activation .....	1
1.1.3. Plasticity and its continuous nature .....	3
1.1.4. Common techniques to investigate macrophage activation .....	3
1.1.4.1. Transcriptomics .....	4
1.1.4.2. Proteomics .....	5
1.1.4.3. Immunoassay-based method .....	6
1.1.5. Modulation of macrophage response .....	6
1.2. Investigating the spatial distribution of activated macrophages .....	7
1.2.1. Immunohistochemistry-Common approach to investigate spatial distribution of markers .....	7
1.3. Mass spectrometry .....	9

1.3.1. Theory.....	9
1.3.2. Ion sources – Matrix Assisted Laser Desorption/Ionization and Electrospray Ionization	10
1.3.3. Mass-to-charge analyzer – Time-of-flight and quadrupole ion trap mass spectrometer ..	11
1.4. Imaging Mass Spectrometry – The transition from 1 to 2 dimensions.....	14
1.5. Approach.....	15
Chapter 2: MALDI of in vitro activated macrophages – Preparation for MALDI IMS.....	17
2.1. Experimental section .....	17
2.1.1. Chemicals and equipment.....	17
2.1.2. Matrix selection, deposition, and general method development .....	18
2.1.3. Explored solvent systems for macrophage extraction .....	19
2.1.4. Sample preparation: Culturing, activation, and harvest of macrophages .....	22
2.1.5. Macrophage work-up protocol – Overview and evolution of lysing technique .....	23
2.1.6. Optional desalting of macrophage lysate .....	26
2.1.7. MALDI-TOF MS system and settings for analysis of mass spectra .....	26
2.2. Results and discussion .....	28
2.2.1. Impact of matrix selection on observed mass spectra .....	28
2.2.2. 2,5-DHB: Macrophage cell dilution experiment and desalting effect.....	33
2.2.3. Effect of extraction solvent and acidity .....	36
2.2.4. Impact of lysing method on observed mass spectra .....	39
2.2.5. Mass spectra of differing activation states in 2,5-DHB .....	39

2.3. Need for separation – transition to LC-MS .....	42
Chapter 3: HPLC-MS of <i>in vitro</i> activated macrophages .....	43
3.1. Experimental section .....	43
3.1.1. Chemicals and equipment.....	43
3.1.2. Preparation of macrophage lysate extract.....	44
3.1.3. LC-MS – Settings and evaluation of system .....	44
3.1.4. Development of HPLC elution protocol.....	45
3.1.5. Preparation of collected fractions for MALDI .....	46
3.1.6. Spectra processing, analysis and evaluation.....	47
3.1.7. Tryptic digestion of collected fractions containing the potential biomarker and preparation for MALDI experiment .....	50
3.1.8. Identification of putative biomarker through peptide sequence database search .....	51
3.1.9. Interpretation of PSD spectra – nomenclature and systematic .....	52
3.2. Results and discussion .....	55
3.2.1. Reproducibility of LC-MS signal intensity .....	55
3.2.2. Analysis of ion signals present under quiescent, IL-4 and LPS-induced condition .....	58
3.2.3. Molecule eluting at minute 21.5 as strong indicator for LPS-induction of macrophages	58
3.2.4. Identification of putative biomarker for LPS-activation as macrophage-capping protein	64
Chapter 4: Summary and future direction.....	71
References.....	74



## List of Figures

Figure 2.1: Overview of mass spectra produced from macrophage lysate spotted with matrices according to Table 2.2. From top to bottom: in 2,5-DHB, “super” DHB, CHCA, SA (dried droplet preparation), and DHAP. The spectra were analyzed as described in 12.1.7. , so only signals with S/N > 100 are labeled (with m/z, or with tick marks), and in this way serve as indicator for spectra quality. ....	30
Figure 2.2: Comparison of reproducibility of cell lysate spotted with sinapinic acid (SA, dried droplet preparation, left), and with 2,5-dihydroxy benzoic acid (2,5-DHB, right). Both sides represent technical replicates prepared with the same sample.....	31
Figure 2.3: Mass spectra of macrophage lysate (NR8383 cells) spotted with 2,5-dihydroxy benzoic acid (1M in 90% methanol, 0.1% trifluoroacetic acid). Spectra recorded in reflectron mode and displayed in the m/z mass range of 900 – 7000 Da (top), and spectra recorded in the linear mode with the m/z range of 1900 – 135000 Da displayed (bottom). The inset depicts an overlay of both modes to demonstrate difference in obtained peak resolution, and to show the preserved fingerprint region, 3900 – 7000 Da, of the NR8383 macrophages. ....	32
Figure 2.4: Amount of macrophage cells needed to produce typical mass spectral fingerprint. Lysate was produced by initial mechanical lysis protocol (trituration), and the resulting lysate was spotted with 2,5-DHB (1M in 90% methanol/0.1% TFA, dried droplet). The lysate was produced from $2.6 \times 10^6$ quiescent macrophage cells, and diluted accordingly so that lysate of $\approx 4400$ cells (top), lysate of $\approx 2200$ cells (2nd), lysate of $\approx 1400$ cells (3rd), and lysate of $\approx 900$ cells (bottom) were applied per dried droplet preparation. The arrow indicates the S/N of the most intense peak in each spectrum.....	34
Figure 2.5: Result of ZipTip® extraction/desalting. Purified macrophage lysate (top), analyte remaining in the extracted lysate (middle), and reference spectra of lysate without ZipTip® extraction.....	35
Figure 2.6: Mass spectra of macrophage cell pellets extracted with differing solvent systems, but producing almost identical mass spectral fingerprint. Extractions solvents were 0.1% n-octyl $\beta$ -glucopyranoside (O $\beta$ G) (top), 50% methanol/0.1% TFA (2nd), 90% methanol/0.1% TFA (3rd), 60% acetonitrile/0.1% TFA (4th), and 90% acetone/0.1% TFA(bottom). All extracts were spotted in dried droplet with 2,5-DHB from 90% methanol/0.1% TFA .....	37

Figure 2.7: Mass spectra of macrophage cell pellets extracted with 2.1% TFA, and spotted in dried droplet with 2,5-DHB from 90% methanol/0.1% TFA. Each spectra represents an individual extraction. It is noticeable that about 2 times more unique peaks (in contrast to Figure 2.3) are present, but the comparison of the independently extracted cell pellets exhibits the lack of reproducibility of these extra peaks. .... 38

Figure 2.8: Overview of three differing lysing techniques: bullet blender (top), freeze thaw (middle), and sonication (bottom). The lysate produced with each technique was spotted with 2,5-DHB in 90% methanol/0.1% TFA, and the obtained spectra exhibit an identical mass spectral fingerprint. .... 40

Figure 2.9: Representative mass spectra of macrophage lysate of quiescent (top), LPS-activated (middle), and IL-4 activated (bottom) cells prepared with 2,5-DHB (1 M in 90% MeOH / 0.1% TFA) in dried droplet technique. All mass spectral fingerprints appear indistinguishable from each other. .... 41

Figure 3.1: LC-MS chromatograms of experiments following the same gradient elution protocol (see Table 3.1) and displayed as total ion chromatogram (TIC, top and middle), and as base peak extracted chromatogram (BPC, top and bottom). The top chromatogram is an overlay of the TIC (rising line) and the corresponding BPC (flat line). This TIC (water injected as sample) demonstrates the raise of the baseline with the increase of acetonitrile in the elution buffer. The chromatograms depicted in the middle (TIC) and at the bottom (BPC) are differential display methods of the same raw data representing a typical LC-MS chromatogram obtained by injecting quiescent macrophage lysate. The insets display a magnified version (minute 11 to 22) of the respective chromatograms. Note: scale difference ..... 49

Figure 3.2: Polypeptide sequence of Alanine(A)-Glutamic acid(E)-Leucine(L)-Serine(S), illustrating b- and y-type ions produced by cleavage of peptide bonds. Brackets are used for E and L to indicate the composition comprising the residual mass of each amino acid along with the respective monoisotopic masses. .... 53

Figure 3.3: Representative base peak chromatograms (BPC) in the range of 0 to 25 minutes of lysates from quiescent (top), LPS activated (middle), and IL-4 activated (bottom) cells. Lysates were prepared according to 3.1.2. and separation was according to elution conditions in Table 3.1. .... 56

Figure 3.4: Representative mass spectra from a LC-MS experiment on quiescent macrophage lysate. The spectra are of the three prominent peaks (see Figure 3.3.) at minute 18.5 min (top), 20.0 min( middle), and 21.5 min (bottom). The ion peaks are additionally labeled with the calculated charge states, and the deconvoluted masses are given as 8451.8 Da (top), 10815.9 Da (middle), and 3990.5 Da (bottom). ..... 61

Figure 3.5: Overlay of extracted ion chromatograms (EIC) obtained from lysate of quiescent (top) and LPS-activated macrophages (5 biological replicates each), demonstrating the absence of the molecule eluting at minute  $\approx$ 21.5. The lysates were separated according to Table 3.1, and the EIC were constructed by integrating all displayed  $m/z$  ( $\pm$  0.5 Da) in Figure 3.4..... 62

Figure 3.6: MALDI mass spectra of macrophage lysate fractions collected at minute 18-19 (top), minute 20-21 (middle), and minute 21-22 (bottom). Ion signals corresponding to the dominant ESI-MS signal (Figure 3.4) are highlighted with a star in the respective spectrum. Lysate fraction were prepared in SA, as described above (3.1.5. )..... 63

Figure 3.7: Overview of representative mass spectra collected on the putative biomarker. The top displays an EIC of lysate from quiescent macrophages with the signal corresponding to the molecule eluting at minute  $\approx$ 21.5 highlighted. The bottom right displays the ESI mass spectrum with the deconvoluted  $m/z$  of 3990.5 Da, while the bottom left depicts an isotopically resolved (ToF in reflectron mode) MALDI mass spectrum of the corresponding dried fraction spotted in SA. The inset of the MALDI spectrum shows the enlarged range from 3974-3996  $m/z$ , exhibiting the monoisotopic peak (3988.4 Da) of the base peak, and an adjacent peak at 3972.39 Da. The difference of 16.0 Da suggests the presence of an additional oxygen atom (=16.0 Da). Note: the mass spectra are of lysate from **quiescent** macrophages, but the absence of this signal serves as indication for LPS-activation..... 67

Figure 3.8: Mass spectrum of tryptic fragments from the digestion experiment on the fraction containing the putative biomarker. The inset contains the sequence fragment (amino acid position 305-339) returned in the MASCOT database search of the depicted spectrum. The theoretical masses of the entire sequence, as well as of both tryptic fragments are indicated. .... 68

Figure 3.9: LIFT spectrum of ion 1375.7 Da (isolation window of  $\pm$  3%) exhibiting mainly b-ion series fragments. The spectrum is annotated with amino acids corresponding to observed mass differences along with the theoretical values of the respective sequences in the inset. Additionally, the dominant peak at 579.1 Da is labeled as the  $y_5$  ion. Ambiguity in assignment is

indicated by providing both potential amino acids. The obtained sequence information supports the proposed sequence for this tryptic fragment. .... 69

Figure 3.10: LIFT spectrum of ion 1601.7 Da (isolation window of +/- 3%) exhibiting y-ion series fragments. The spectrum is annotated with amino acids corresponding to observed mass differences along with the theoretical values of the respective sequences in the inset. The obtained sequence information supports the proposed sequence for this tryptic fragment. .... 70

## Glossary

1,5-DAN	1,5-diaminonaphthalene
2,5-DHAB	2,5-Dihydroxyacetophenone
2,5-DHB	2,5-Dihydroxy benzoic acid
BPC	Base peak chromatogram
CHCA	$\alpha$ -cyano-hydroxy cinnamic acid
EIC	Extracted ion chromatogram
ESI	Electrospray ionization
IL-4	Interleukin-4
ISD	In-source decay
LPS	Lipopolysaccharide
MALDI	Matrix assisted desorption/ionization
M1	Classical activated macrophage phenotype
M2	Alternatively activated macrophage phenotype
M(IL-4)	Macrophage population treated with interleukin-4
M(LPS)	Macrophage population treated with the endotoxin Lipopolysaccharide
MeOH	Methanol
RSD	Relative standard deviation
SA	4-hydroxy cinnamic acid, "sinapinic acid"
TIC	Total ion chromatogram
ToF	Time-of-Flight (type of mass spectrometer)
tof	time-of-flight (equation)
TFA	Trifluoro acetic acid

TLR-4	Toll-like receptor 4
TNF- $\alpha$	Tumor-necrosis factor alpha

## Chapter 1: Background and Significance

### 1.1. The Macrophage

#### 1.1.1. A cell type with many functions

In mammals, the macrophage is a cell type that is widely distributed throughout the organism, and can be found in every organ, and in most tissues.<sup>1,2</sup> The precursor cells, monocytes, are released into the circulatory system by the bone marrow, and differentiate into macrophages upon migration into tissue.<sup>3</sup> The term “macrophage” (greek, from *makros* "large" and *phagein* "eat") was originally coined by Elie Metchnikoff based on his observation that many microorganisms could be engulfed and digested by large mononuclear phagocytic cells.<sup>4</sup> Though commonly regarded as only part of the innate immune system, it was later discovered that macrophages are highly adaptive, versatile cells involved in a wide variety of biological processes.<sup>2</sup> These include host defense, immune regulation, as well as the orchestration of wound healing and other homeostatic tasks.<sup>1,5</sup> In response to the local microenvironment, macrophages assume protective functions as in antimicrobial defense, in homeostatic or restorative roles as in the wound healing process, and also in pathogenic functions, e.g. in tumorigenesis, autoimmunity, or allergy and asthma.<sup>3</sup>

#### 1.1.2. Macrophage activation

The distributed tissue-resident macrophages are remarkable in that they display a high degree of plasticity, i.e. they can change their physiology based on chemical and physical cues from their microenvironment.<sup>1,6</sup> This process is called activation, and is defined as the perturbation of macrophages by exogenous agents other than via the basal tissue microenvironment exposure.

These cues include the broad category of signaling proteins called cytokines, as well as other modulators like the presence of cell debris and the phagocytosis of proximate cells.<sup>7</sup>

The most prominent<sup>1</sup> example of a microbial structure to trigger a physiologic response in macrophages is lipopolysaccharide (LPS), a cell-wall component of Gram-negative bacteria. It has been known since the late 1800's<sup>8</sup> to induce a strong reaction in affected organism.<sup>4</sup> The presence of LPS is detected by a transmembrane receptor, the Toll-like receptor 4 (TLR-4), on the macrophage surface. The detection triggers an intracellular cascade leading to the formation and release of antimicrobial peptides, the secretion of signaling molecules (particularly the cytokine tumor-necrosis factor (TNF)), as well as to increased phagocytic activity and the efficient production of effector molecules (reactive oxygen and nitrogen intermediates). This particular stimulation of macrophages is referred to as *classical* activation.<sup>4,9</sup>

In 1992, Stein et al. presented their work on an *alternative* activation state of macrophages induced through the treatment with the cytokine interleukin-4 (IL-4). They observed that, in contrast to classical activated macrophages, the secretion of proinflammatory cytokines was reduced and the capacity for endocytic clearance of mannosylated ligands was strongly enhanced.<sup>10</sup> This activation through IL-4 was later associated with a wound healing macrophage phenotype.<sup>11-13</sup>

To parallel the nomenclature of T helper cell polarization, the *classical* and *alternative* macrophage activation state are widely referred to as M1 and M2 respectively,<sup>14</sup> whereas the category of M2 grew over time with the discovery of more, distinct activation states to be divided further into subcategories<sup>9</sup> (activation states are sometimes also referred to as polarization states).<sup>7</sup>



Following a recent attempt in the field of macrophage activation to reorganize and clarify experimental conditions and results,<sup>7</sup> this thesis will follow the suggested guidelines to label LPS treated macrophages as M(LPS) as well as the macrophages treated with IL-4 as M(IL-4).

### 1.1.3. Plasticity and its continuous nature

Not only do distinct states of macrophages exist, it could also be shown that the functional phenotype of activated macrophages can be reversibly shifted with the help of different stimuli.<sup>15-19</sup> Expanding on the observation of this plasticity, Mosser *et al.* suggested that macrophages can exist along a continuum in between three fundamental functions: host defense, wound healing, and immune regulation. Illustrating this with a color wheel of macrophage polarization, they argue that the function of activated macrophages exist as shades in between these primary tasks.<sup>13</sup> Consequently, the presence and quantity of biomarkers associated with macrophage phenotypes has to be determined to gain insight into the current, predominant function of the investigated macrophage population.

### 1.1.4. Common techniques to investigate macrophage activation

Macrophages have the ability to synthesize proteins to maintain cellular functions and to perform tasks associated with their activation state. Proteins, also known as polypeptides, consist in the simplest form of a chain of amino acids, and are produced in two major steps. During the first step, the transcription, the genes on the macrophage's DNA are transcribed into corresponding RNA, which can be processed further to messenger RNA (mRNA). The encoded information in the mRNA is then used in the second step, the translation, as a template for the assembly of the polypeptide.<sup>20</sup> These sequential steps are inherently tied to the synthesis of

proteins, and so the activation state of macrophages can be explored by targeting the RNA<sup>21-24</sup> and/or the polypeptide<sup>25-29</sup> level of this process.

Both approaches, targeting the products of transcription or those of translation, are referred to as the field of transcriptomics and proteomics, respectively, and have also been used to investigate macrophages.<sup>30,31</sup> The ‘omics’ in both terms imply that the aim is to capture virtually all molecules of the respective category of an investigated organism under specified conditions, and the evaluation of these data sets can grant insights into the inner workings of biological processes.<sup>32</sup>

#### 1.1.4.1. Transcriptomics

The expression of RNA, the transcriptome, is typically monitored and quantified using the high-throughput technique of DNA microarrays.<sup>33</sup> In this procedure, the extracted and purified RNA sample is fluorescently labeled during reverse transcription, and then incubated on a chip containing thousands of counter strands of DNA representing genes from the investigated organism. During this incubation, complementary nucleic acid strands hybridize, and, after a washing step to remove the weaker, non-specific adsorbed analytes, the identity and the quantity of the analyzed RNA can be determined by the location and intensity of the fluorescent signal.<sup>34</sup> Some of the limitations of this technique include that the preparation of the counter strand DNA, the so-called probes that are applied to the chip during the manufacturing of the microarray, are very labor intensive in the preparation, and the sequence information for them should, at best, be derived from a complete genomic database of the investigated organism.<sup>34</sup>

#### 1.1.4.2. Proteomics

The polypeptides synthesized during the second step, the translation, are typically analyzed by high-performance liquid chromatography (HPLC or short LC) mass spectrometry (MS), in which a complex mixture of polypeptides is separated through the LC, and the eluting sample subjected to mass spectrometry. By choosing from a wide variety of separation columns and elution conditions, the LC can separate polypeptides according to inherent characteristics like mass, hydrophobicity, or biospecificity. The eluting analyte can either be directly subjected to mass spectrometric analysis through interfacing the LC with a MS through an electrospray ionization (ESI) interface, or the eluting fractions can be collected, and after further processing subjected to MS via matrix-assisted laser desorption ionization (MALDI).<sup>35</sup> To render a large mass range accessible to the mass spectrometric analysis, the analyte mixture is commonly proteolytic digested to form peptide fragments,<sup>36</sup> which are in a mass-to-charge range (<20 kDa) amenable to routine mass spectrometric analysis.<sup>37</sup> Mass spectrometry is predominantly regarded as semi-quantitative in nature, since the ionization efficiency of the analyte is governed by inherent characteristics of the analyzed compound, and this efficiency is additionally confounded by suppressive/enhancing matrix effects. Hence, a widespread accepted method to obtain quantitative information is the use of isotope-labeled reference peptides as internal standard.<sup>35,37</sup> LC-MS based analysis employing the sample digestion step, however, suffer from inadequate identification of polypeptides arising from alternative splicing. These isoforms of polypeptides share a high percentage of amino acid sequence, and thus proteolytic fragments lose specificity in the identification process.<sup>38,39</sup>

#### 1.1.4.3. Immunoassay-based method

Another technique to investigate the activation state of macrophages is based on the highly specific antigen-antibody reaction. Cytokines that are released upon macrophage stimulation are routinely detected, and quantified through enzyme-linked immunosorbent assays (ELISA).<sup>40</sup> The ELISA is a wet-lab based technique that uses the catalytic activity of an enzyme to convert a substrate into a product which can be spectrophotometrically quantified.<sup>41</sup> This enzymatic signal amplification allows for low detection limits, but the use of antibodies to capture specific analytes limits this technique to the detection/quantification of specified target molecules, so that no exploratory experiments with unknown biomarkers can be conducted with this technique.<sup>1</sup>

#### 1.1.5. Modulation of macrophage response

Uncovering the many functions of macrophages in the body also revealed connections between diseases and macrophage subsets.<sup>3,42,43</sup> Unrestrained macrophage activity can be linked to chronic inflammation,<sup>44</sup> fibrosis,<sup>45,46</sup> metabolic disease<sup>47</sup> or the proliferation of cancerous tissue.<sup>48,49</sup> A further, not disease-related field in which alteration of macrophage function is desirable, is the realm of medical implants and tissue regeneration after surgery. Here, the promotion of tissue repair as opposed to triggering foreign body reaction is the desired outcome.<sup>50,51</sup>

Targeting the activation state of macrophages with effector molecules is a promising approach in resolving complications caused by dysregulated<sup>13</sup> macrophage populations<sup>18</sup> or to ameliorate the impact of surgery and medical implants.<sup>51</sup>

## 1.2. Investigating the spatial distribution of activated macrophages

As described above, there are instances in which the modulation of the macrophage response is desired (e.g. to counter chronic inflammation, or to protect implants from encapsulation). As pointed out by Stein et al,<sup>17</sup> the biological microenvironment of macrophage populations decisively influence the observed functional phenotypes, so it is desirable to conduct in vivo experiments where the modulation agent is administered locally into the investigated tissue. Consequently, unaltered tissue portions of the model organism can be investigated in a side-by-side approach, and hence would serve as an internal standard that adjusts for biological variability observed in between subjects. Additionally, the spatial distribution (e.g. proximity to damaged tissue, or distance to the source of the modulator) of macrophage populations can be analyzed and interpreted within the biological context.

To this end, the discussed transcriptomics and proteomic experiments, although yielding abundant information on macrophage activation states, are impracticable with respect to the amount of individual experiments that would have to be performed on small sections of a tissue section. To answer general questions regarding spatial distribution of specific target molecules on tissue samples, the well-established analytical tool of immunohistochemistry is commonly applied.<sup>52</sup>

### 1.2.1. Immunohistochemistry –Common approach to investigate spatial distribution of markers

Immunohistochemistry is an analytical tool that uses the high specificity of the antibody-antigen reaction to locate and highlight (through conjugated fluorophores or via radio labeling) the location of target molecules on tissue sections. Several steps are necessary to prepare a sample for analysis: after explantation, the tissue sample is typically fixed through the use of formalin cross-linking of the present biomolecules, followed by embedding in paraffin to

conserve the structural integrity. After sectioning the tissue into 5-15  $\mu\text{m}$  thick slices and transferring these to glass slides, the tissue sections are typically pre-treated to expose the analyte for the following labeling step. The pre-treatment step aims to reduce the initially induced cross-linking, and thus make the sample more porous so that the labeling antibody can more easily diffuse into the tissue and bind to the detection region, the epitope, on the antigen. This reduction can be achieved through protease digestion, which can cleave proteins that are incorporated into the cross-linked network, or through a technique called antigen retrieval, in which the epitopes are rendered more accessible by heat-induced protein unfolding.

After the preparation of the tissue section, the actual step of immunochemically targeting the analyte is performed. This is a two-step procedure, in which the tissue is first incubated with a primary antibody expressed in a certain host (e.g. mouse, rabbit, goat, etc.) to selectively bind to the molecule of interest, followed by the incubation with a secondary antibody targeting antibodies derived from certain species (i.e. targeting mouse, rabbit, goat antibodies). Additionally, the second antibody is conjugated to a reporter system like a fluorophore or an enzyme that can convert its substrate into fluorescent product. The fluorescence of either reporter system can then be used to obtain the spatial distribution of the targeted molecule with the help of fluorescence microscopy.<sup>52</sup>

This method is widely accepted as tool in research and diagnostics, which is also reflected by an increasing number of available primary antibodies from various host animals, and it has also been used to investigate the distribution of activated macrophages.<sup>53</sup> However, as Nuovo details,<sup>52</sup> there are various challenges and pitfalls that affect the quality of the obtained data. Among these, it is emphasized that an optimized protocol for detecting a specific analyte in one tissue section may not give rise to any signal at all when investigating a different type of tissue

despite the presence of analyte. There is no *a priori* way to tell which tissue pre-treatment method will improve the observed signal, or, in the worst case, could even result in complete loss of it. During the lengthy multistep sample preparation, numerous steps are critical for the observed overall result, so that the obtained results are best interpreted in comparison to samples prepared side-by-side. Additionally, the commercial availability and specificity of primary antibodies may not be given for the molecule of interest. To exacerbate this situation, the inherent requirement of the employed two-antibody-system severely limits the amount of different analyte that can be detected simultaneously on one tissue section (i.e. the selection of species from which the primary antibodies are derived translates into what species-specific secondary antibodies can be used without confounding the observed results). A similar problem also arises from the requirement that the emitted fluorescence of the used reporter system cannot spectrally overlap. The availability of suitable absorption/emission wavelengths of laser-fluorophore-systems that can be used adds a similar constraint like the two-antibody-system to the number of simultaneously detectable analytes.

To this end, an emerging technology extending the technique of mass spectrometry to analyze spatial analyte distribution could overcome certain limitations of immunohistochemistry.

### 1.3. Mass spectrometry

#### 1.3.1. Theory

Mass spectrometry is a technique to determine the molecular mass of molecules and atoms by measuring the mass-to-charge ( $m/z$ ) ratio of the respective ionized species. It can either directly provide the elemental composition of the analyzed material in the case that the determination of  $m/z$  is accurate enough so that only one combination of atomic masses (more exactly, of the isotopes) can lead to the observed  $m/z$ , or provide this information indirectly by

analyzing fragments of the (intentionally) fragmented ion of interest. Additionally, analyzing those fragments can provide structural information on the investigated substance. Conceptually, a mass spectrometer consists of an ion source, a mass-to-charge analyzer, and an ion detector.

### 1.3.2. Ion sources – Matrix Assisted Laser Desorption/Ionization and Electrospray Ionization

The task of the ion source is to generate charged analyte molecules. Additionally, these ions have to be in the gas phase so that they can be separated according to their  $m/z$  with the help of electrical and/or magnetic fields.<sup>37</sup>

The technique called matrix assisted laser desorption/ionization (MALDI)<sup>54</sup> enabled the production of mostly singly charged gas phase ions of large, nonvolatile, and potentially labile molecules with little or no fragmentation of the parent ion from solid analyte. This effect, called soft ionization, allowed the investigation of intact, non-volatile biopolymers of molecular weights >1500 Da. Although some fundamental aspects of the mechanism are still subject to research, a large body of experimental guidelines for successful MALDI experiments has emerged over time.<sup>37,55</sup> Typically, the analyte is mixed with a large excess of an organic matrix compound, ranging from an empirical-derived molar analyte-to-matrix ratios of 1:100 to 1:10,000,000, and is most commonly co-deposited on a metal target from solution. For most experiments, the dried co-crystal is then inserted into a medium to high vacuum ( $10^{-7}$  to  $>10^{-9}$  mbar) mass spectrometer, and the sample is irradiated with short pulses of laser light to generate a plume containing ionized species that is then subjected to the mass spectrometric analysis. Typically, nitrogen lasers (wavelength of 357 nm) or Nd:YAG lasers (wavelength of 355 nm when the 3<sup>rd</sup> harmonic is used) are used with ultra-violet light absorbing matrices, and CO<sub>2</sub> lasers are used with matrices that absorb in the infrared range (bands of wavelengths around 9.4  $\mu\text{m}$  and 10.6  $\mu\text{m}$ ). Although models attempting to predict ionization efficiency of certain analyte



classes, e.g. based on properties like gas-phase basicity, have been proposed, no model can capture the entirety of the this complex process.<sup>56</sup>

The second major soft ionization technique is called electrospray ionization (ESI). In contrast to MALDI, it produces stable gas phase ions from dissolved analyte. The ions are generated by spraying a solution of analyte into an electric field. Only polar solvents are compatible, since non-polar solvents lack the required conductivity necessary to produce charges through electrochemistry. The initially generated charged, fine droplets disintegrate to smaller droplets through increasing repulsive columbic forces as the solvent evaporates. After complete desolvation of the non-volatile analyte, the resulting ion is typically multiply charged, which, in contrast to singly charged ions from MALDI, allow for the observed mass-to-charge ratio to fall into the range (< 20kDa) of most commonly used mass spectrometers, and thus allowing the analysis of larger molecules than MALDI.<sup>37</sup>

### 1.3.3. Mass-to-charge analyzer – Time-of-flight and quadrupole ion trap mass spectrometer

The ions produced in the ion source are then separated spatially and/or temporally in the mass-to-charge analyzer before they are detected. To illustrate this, both employed mass spectrometer will be briefly discussed.

In a time-of-flight (ToF) instrument, the generated ions are extracted from the source into a field free drift tube by the application of a pulsed acceleration potential on the order of 25-35 keV.

**Equation** 1.1 shows how this potential,  $V$ , is related to the resulting velocity,  $v$ , through the number of charges,  $z$ , the elementary charge,  $e$ , and the ion mass,  $m$ :

$$zeV = \frac{1}{2} m v^2$$

*Equation 1.1: Kinetic energy of ions after acceleration*

*Re-arranging*

Equation 1.1 as in Equation 1.2 demonstrates the inverse quadratic relationship between the ion velocity and the  $m/z$ .

$$v = \left( \frac{2 z e V}{m} \right)^{\frac{1}{2}}$$

*Equation 1.2: Re-arranged equation 1 to show inverse quadratic dependence of  $v$  to  $m/z$*

To obtain the time-of-flight (tof), i.e. the time it takes the ions packages to travel from the source to the detector, the instrument-specific geometric factor  $L$  is used according to the definition of velocity as in **Equation 1.3**:

$$tof = \frac{L}{v} = L \left( \frac{m}{2 z e V} \right)^{\frac{1}{2}}$$

*Equation 1.3: Relation of time-of-flight (tof) to the mass-to-charge ( $m/z$ ) of the timed ions*

Ideally, all ions experience the same acceleration potential, and separate during their travel through the field free drift tube according to their  $m/z$ , and are detected after their respective time-of-flight (tof).<sup>37</sup>

This basic concept of time-of-flight measurements, generally referred to as linear ToF mode, can be enhanced to address a spread in tof of ions of the same  $m/z$  caused by spatial and velocity distributions of the initial ion packet. The underlying distribution in kinetic energies can be compensated by reflecting the traveling ion packets with the help of an ion mirror onto a

secondary ion detector. In this so-called reflectron ToF mass spectrometer, ions of identical  $m/z$  but higher kinetic energy penetrate deeper into the ion mirror before being reflected, and hence travel a slightly longer distance. The instrument is constructed in way that the secondary detector is placed at the electronic focus plane of the mirror to benefit from the reduction in spatial distribution of the traveling ion packets.<sup>37</sup>

Typically, a reflectron ToF mass spectrometer can be run in linear mode, in which the reflectron is deactivated and the ions are detected with a primary detector located behind the ion mirror, or in the reflectron mode, which allows for a lower spread in tof, and hence a better resolution of arriving ion packets.

Additional to the focusing effect of the reflectron, it can also be used to observe fragment ions from post-source decay (PSD). PSD refers to the behavior of ions to dissociate after the acceleration of the ion packages, during the travel in the field free drift tube, but before reaching the reflectron.<sup>57</sup> The ions travel at a certain velocity based on their initial mass, but will separate according to their new, reduced  $m/z$  when a second acceleration potential is applied. The so-called LIFT mode of the Ultraflex III ToF/ToF (Bruker Daltonics) is based on this principle, and thus allows analyzing desorbed ions further by exploring the fragments produced through PSD.<sup>58</sup>

Another mass-to-charge analyzer is the 3D quadrupole ion trap (QIT). Here, the ions generated in the source are stored in a quadrupole electric field generated by applying a radio frequency (RF) potential to a ring electrode. The trapped ions are collisionally cooled through inert buffer gas like nitrogen to reduce the amplitude of their random displacement from the  $m/z$  specific orbit that they assume. The ions oscillate on concentric three-dimensional orbits according to their  $m/z$  and the applied RF potential. Through ramping the amplitude of this potential, ions of increasing  $m/z$  are sequentially ejected from the trap and are registered through

their impact on a detector. The  $m/z$  can be determined from the necessary RF amplitude for the ejection, and achievable separation of ions of different  $m/z$  is, among others factors, a combination of the scan speed of this amplitude and the detection speed of the detector. A constraint for the amount of ions that can be detected simultaneous is imposed by the so-called space-charge effect. This effect, in which the oscillating ion packets perturb each other's orbit, limits the charge density that can be achieved in a QIT. This problem is addressed by measuring the ion flux in an initial pre-scan, followed by adjustment of the ionization time to produce a target amount of ions (depending on manufacture, this is called automatic gain control (AGC) or ion-current control (ICC)).

#### 1.4. Imaging Mass Spectrometry – The transition from 1 to 2 dimensions

Imaging mass spectrometry (IMS) is the application of mass spectrometric methods to spatially distributed samples like thin biological tissue sections. This is essentially achieved by probing a surface in an x,y-fashion, and was driven by technological advancement of the mass spectrometric field with respect to acquisition speed of traditional mass spectra, as well as innovations aiming at conservation of information of spatial distribution of analytes.<sup>59</sup> The major advantage of this approach lies in the ability of mass spectrometry to measure hundreds of different ions simultaneously without the need for molecular tags as in labeling for immunohistochemistry, and it is therefore also suited for exploring a sample without *a priori* knowledge of composition.<sup>60</sup> Particularly, the combination of MALDI with IMS offers the advantage of providing information of spatial distribution of small molecules like drug metabolites up to large, intact proteins of up to 100 kDa.<sup>61</sup> According to Goodwin is “[t]he upper limit for reasonably sensitive detection [...] currently around 25-30 kDa”, since MALDI tends to generate only singly charged ions, but on-sample enzymatic digestion can provide indirect

information on larger proteins.<sup>62</sup> Techniques like desorption electrospray ionization (DESI) additionally aim at combining the advantage of multiply charged ions as commonly observed in electrospray ionization with the ability to scan a surface under atmospheric conditions.<sup>63</sup>

### 1.5. Approach

The following chapter describes the experiments conducted with MALDI MS in preparation of MALDI IMS for macrophage activation studies. The scope of this work was to establish a robust method to distinguish the activation state of macrophages on explanted tissue sections. To this end, an *in vitro* activated immortalized macrophage culture was used as a readily accessible model to test combinations of lysis and sample preparation protocols to find suitable biomarkers that allow the unambiguous identification of the induced activation state. For this, the well-established approach of mass spectral fingerprinting<sup>37</sup> was employed, which has been demonstrated to allow reproducible identification of bacteria down to the strain level.<sup>64</sup> Also mammalian cell lines, which exhibit a less stable MS fingerprint,<sup>65</sup> could be rapidly characterized and cross-contamination of cultured cell lines could be readily distinguished with this technique,<sup>66</sup> suggesting mass spectral fingerprinting to be a suitable approach. It should also be noted that Quedraogo et al. published data on MALDI-TOF MS of activated macrophages (human), claiming that “The fingerprints induced by the M1 agonists, IFN- $\gamma$ , TNF, LPS and LPS + IFN- $\gamma$ , and the M2 agonists, IL-4, TGF- $\beta$ 1 and IL-10, were specific and readily identifiable.”<sup>67</sup> However, central claims, like the identification of peaks at  $m/z$  of 6827 or 6826 as related to the activation state M1, while peaks at  $m/z$  6835 or 6833 are supposed to indicate activation state M2, are in contrast to the author’s criteria for similarity across spectra of a 2000 ppm  $m/z$  window, which would encompass all the claimed different  $m/z$  values. Further, none of the ions representing these biomarkers were identified, so supporting the claim of distinguishing

activation states cannot be placed into the biological context, which would give the claim more weight. Among other inconsistencies, the author further omits crucial information on the sample preparation process like the solvent that was used to prepare the MALDI matrix, as well as the matrix concentration, rendering this publication an unreliable source for own experiments.

## **Chapter 2: MALDI of in vitro activated macrophages – Preparation for MALDI IMS**

As discussed in Chapter 1, mass spectrometry-based proteomic experiments suggest an abundant array of biomarkers for macrophage activation states. However, these biomarkers were identified in elaborate experiments involving several steps that reduced the complexity of the investigated sample. The advantage of the MALDI approach, on the other hand, is its simplicity and reproducibility. As described above, though, the ionization efficiency of analytes cannot be predicted, so the majority of tested experimental conditions are based on loose guidelines derived from previous experiments reported in the literature.

### 2.1. Experimental section

#### 2.1.1. Chemicals and equipment

2,5-dihydroxybenzoic acid (2,5-DHB, 99% purity), 1,5-diaminonaphthalene (1,5-DAN, 97% purity), 2-hydroxy-5-methoxy benzoic acid (99% purity), 2,5-dihydroxyacetophenone (2,5-DHAB, 98+% purity), diammonium hydrogen citrate (99+% purity), and trifluoroacetic acid (TFA, 99% purity) were purchased from Alfa Aesar (Ward Hill, MA, USA). 3,5-dimethoxy-4-hydroxy cinnamic acid (sinapinic acid, SA, 98% purity), and  $\alpha$ -cyano-4-hydroxycinnamic acid (CHCA, 97% purity) were purchased from Acros Organics (Geel, Belgium). The solvents acetonitrile (HPLC grade), and methanol (HPLC grade) were from EMD Millipore (Billerica, MA, USA), ethanol (USP grade) from Koptec (VWR, Radnor, PA, USA), and de-ionized water (HPLC grade) were purchased from Thermo Fisher Scientific (Waltham, MA, USA). The MALDI targets with non hydrophobic surface were purchased from Hudson Surface Technology (Fort Lee, NJ, USA). ZipTip® (OMIX 96 C18, 100  $\mu$ L) were obtained from Agilent Technologies (Santa Clara, CA, USA).

For the cell culture, the immortalized macrophage cell line NR8383 (rat, alveolar, CRL-2192), and the F-12 K medium (Kaighn's modification of Ham's F-12 medium) were purchased

from ATCC (Manassas, VA, USA). Fetal bovine serum (regular, heat inactivated) was purchased from Corning/Mediatech (Corning, NY, USA), and antibiotic antimycotic solution (100x, stabilized) was obtained from Sigma Aldrich (St. Louis, MO, USA). The cytokine interleukin-4 (IL-4, recombinant, rat, 25 µg) was obtained from R & D systems, Inc. (Minneapolis, MN, USA), and lipopolysaccharide (LPS, salmonella typhimurium) was purchased from EMD Millipore (Billerica, MA, USA).

### 2.1.2. Matrix selection, deposition, and general method development

Matrices were chosen based on suggested<sup>37</sup> application to investigate small (<10 kDa) proteins/peptides ( $\alpha$ -cyano-hydroxy cinnamic acid, CHCA), and heavier (>10 kDa) proteins (3,5-dimethoxy-4-hydroxy cinnamic acid, “sinapinic acid”, SA), as well as the all-round matrix 2,5-dihydroxy benzoic acid. In an attempt to investigate potential larger molecules than the postulated sensitivity cut off of 25-30 kDa,<sup>62</sup> two additionally matrices were investigated: 1,5-diaminonaphthalene (1,5-DAN) is known to promote in-source decay (ISD),<sup>68</sup> which allows identification of larger proteins through the detection specific fragments, and which was demonstrated in MALDI IMS experiments on tissue sections (parent ions up to 70 kDa).<sup>69,70</sup> The matrix 2,5-dihydroxyacetophenone (2,5-DHAB) promotes the generation of multiply charged ions from MALDI,<sup>71</sup> so it was tested for its ability to reduce the  $m/z$  of larger ions by increasing the charge.

For the deposition of matrix/analyte onto the stainless steel MALDI target, three standard methods were investigated: The simple “dried droplet”,<sup>72</sup> where the matrix and analyte are mixed in solution before spotting, along with the related “fast evaporation” technique,<sup>73</sup> where the matrix is pre-spotted to form very fine crystals during solvent evaporation (seconds to a few minutes) prior to the application of dissolved analyte, and the “sandwich” technique, a



modification of the fast evaporation technique, wherein an additional layer of matrix solution is applied on top of the dried matrix-analyte layers.

The method development was conducted in an iterative way, in which changes to the preparation protocol were tested side-by-side with previously established protocols. The resulting mass spectra were then compared and inspected for its information density (i.e. ion signal density of differing  $m/z$ ), reproducibility, and for potential biomarkers (in case sample derived from differentially activated macrophages was investigated, see below). All tested combinations were usually spotted in three technical replicates, and in at least three analyte-to-matrix-ratios. Since the sample here is generally a complex mixture without a known concentration of its individual components, the mixing ratio of analyte-to-matrix was varied by variation of proportion of mixed volumes of matrix and analyte solution. Further, new methods were tested with readily available non-polarized (i.e. quiescent) NR8383 macrophages, and, if MS spectra suggested that additional information (compared to the established procedure) could be obtained, the method was repeated with the lysate of polarized macrophages. *Table 2.2* displays a selection of preparation methods with the respectively, most commonly, used matrix concentrations, employed solvent system, and application techniques.

### 2.1.3. Explored solvent systems for macrophage extraction

In an attempt to investigate the impact of extraction solvent on the observed mass spectra, aliquots of approximately  $1 \times 10^6$  quiescent macrophages each were extracted with 100  $\mu$ L of various solvent systems. The hypothesis was that molecules could be differentially extracted based hydrophobicity, and hence the observed mass spectra would be altered to display differing groups of analytes. All samples were prepared with 2,5-DHB (1M, 90% methanol, 0.1% TFA) in the dried droplet preparation. The choice of investigated solutions was loosely based on solvents

commonly employed in MALDI matrix preparations. Further, the impact of acidity of the solvent system on the extraction was explored by comparison of extractions performed with 0.1 % (v/v) TFA, and 2.1 % (v/v) TFA. *Table 2.1* depicts the tested extraction solvents.

*Table 2.1: Overview of solvent systems explored for macrophage extraction*

<b>Solvent</b>	<b>Additive</b>
water	n-octyl $\beta$ -glucopyranoside (O $\beta$ G), 0.1% (w/w)
water	trifluoro acetic acid (TFA), 0.1% (v/v) and 2.1% (v/v)
methanol (50% (v/v) in water)	TFA, 0.1% (v/v)
methanol (90% (v/v) in water)	TFA, 0.1% (v/v)
acetonitrile (60% (v/v) in water)	TFA, 0.1% (v/v)
acetonitrile	TFA, 0.1% (v/v)
acetone (90% (v/v) in water)	TFA, 0.1% (v/v)

Table 2.2: Selection of matrix molecules and preparation conditions investigated in the direct MALDI of macrophage lysate

Matrix	Concentration/solvent	Application technique
<i>2,5-dihydroxy benzoic acid</i>	1 M in 90% methanol, 0.1% TFA	dried droplet
	1 M in 33% (acetonitrile/H <sub>2</sub> O, 0.1% (v/v) TFA in H <sub>2</sub> O)	
<i>"super" 2,5-dihydroxy benzoic acid</i> (= 9:1 (w/w) ratio of <i>2,5-dihydroxy benzoic acid</i> to <i>2-hydroxy-5-methoxy benzoic acid</i> )	50 mg per mL in 50% (acetonitrile/H <sub>2</sub> O, 0.1% (v/v) TFA in H <sub>2</sub> O)	dried droplet
<i>α-cyano-hydroxy cinnamic acid</i>	saturated, in 30% (acetonitrile/H <sub>2</sub> O, 0.1% (v/v) TFA in H <sub>2</sub> O)	dried droplet
<i>3,5-dimethoxy-4-hydroxy cinnamic acid</i> ( <i>"sinapinic acid"</i> )	0.1 M in 90% methanol, 0.1% TFA	dried droplet
	target pre-spotted with saturated solution (in ethanol); sample mixed 1:1 with 30% (acetonitrile/H <sub>2</sub> O, 0.1% (v/v) TFA in H <sub>2</sub> O)	layer technique
<i>1,5-diaminonaphthalene</i>	saturated, in 50% (acetonitrile/H <sub>2</sub> O, 0.1% (v/v) TFA in H <sub>2</sub> O)	dried droplet
<i>2,5-dihydroxyacetophenone</i>	0.133 mol/L in ethanol, mixed 3:1 with 0.08 mol/L diammonium hydrogen citrate (acidified with 2% TFA solution (1:1) prior to deposition)	dried droplet

#### 2.1.4. Sample preparation: Culturing, activation, and harvest of macrophages

The immortalized macrophage cell line NR8383 (*rattus norvegicus*; alveolar) was obtained from the American Type and Culture Collection (ATCC), and the macrophages were cultured according to the protocol described by Helmke et al.<sup>74</sup> Briefly, the macrophages were incubated at 37°C in a Ham's F12K medium containing 15% fetal bovine serum and 1% antibiotic/antimycotic solution. The medium is changed about twice a week, and cultures are split occasionally when the culturing flask wall appeared to be covered with attached cells.

The process of changing the media consisted of retrieving the nutrient-depleted media from the culture flask, and replenishing the flask with fresh complete media. The retrieved media contains floating macrophages (approximately half of the present cell population),<sup>75</sup> which are concentrated into a cell pellet by centrifuging at 140-250 g for 10 min (supernatant is decanted). These macrophages were either used for activation experiments as described in the following paragraph, or directly processed for experiments on quiescent macrophages (washed once with 100 µL of HPLC grade water and further processed as described in the macrophage work-up protocol section). Either way, the macrophage counts were generally estimated with the help of an automated cell counter, Invitrogene Countess<sup>TM</sup>, based on the technique of staining with trypan blue.<sup>76</sup> For this, a sample of 20 µL of the re-suspended pellet was mixed with 20 µL of the trypan blue dye, and the mixture was analyzed according to manufacturer's instructions. In the case of activation experiments, the cell pellets were re-suspended in 5 mL of complete media, the macrophage count was established, and the sample were further diluted to yield approximately  $5 \times 10^5$  macrophages/mL.

These sub-samples of the harvested NR8383 macrophages were treated once with the endotoxin lipopolysaccharide (LPS) at a concentration of 200 ng per mL of cell suspension,

while for the induction of the M(IL-4) state, sub-samples of similar cell count were treated with the cytokine interleukin-4 (IL-4) at a concentration of 50 ng per mL of cell suspension.<sup>77</sup> While the M(LPS) state is reached within 24h (detected by the release of the cytokine tumor necrosis factor alpha (TNF $\alpha$ )<sup>78</sup>), the cell culture had to be treated repetitively each day for 2 days to detectably form M(IL-4) (confirmed by the production of the cytokine interleukin-10 (IL-10), the absence of TNF, and low levels of IL-6, as detected in an ELISA assay).

#### 2.1.5. Macrophage work-up protocol – Overview and evolution of lysing technique

Starting with a mass-spectrometry sample-preparation method for chicken macrophages,<sup>79</sup> the protocol was modified in a systematic way. Major changes (e.g. changing the lysing method) were evaluated based on reproducibility and information density of the obtained mass spectra, and new methods were compared with preparation procedures previously established. To minimize the impact of biological variability on this iterative process, previous and the new procedure were performed side-by-side on subpopulation of the same batch of harvested macrophages. Initially, the results on quiescent macrophages were evaluated, before polarized macrophages were investigated. *Table 2.3* gives a chronological (top to bottom) overview of the explored sample preparation methods.

The initial lysing technique consisted of trituration of macrophage cell pellets in a small amount (40-200  $\mu$ L) of 0.01%-0.1% (w/v) n-octyl  $\beta$ -glucopyranoside solution (a non-ionic detergent).<sup>79</sup> Based on the observation that the macrophage pellets could be extracted multiple times to obtain sample solution that would produce similar mass spectra, it was concluded that the cell lysis was incomplete, so a more rigorous and reproducible automatic mechanical lysing protocol involving a bullet blender<sup>®</sup><sup>80</sup> was investigated. Further, two freeze-thaw protocols,<sup>81,82</sup> an ultra-sonication approach, and finally a lyophilization procedure were explored, and the

obtained MALDI spectra were compared to determine the most effective, reproducible procedure that maximized obtained signal intensity and amount of unique ions of differing  $m/z$ .

As basis to evaluate new lysing methods, the generally well-established and preparation-insensitive<sup>83</sup> matrix *2,5-dihydroxy benzoic acid* ( $c=1\text{mol/L}$ ) in 90% methanol (0.1% (v/v) *trifluoroacetic acid*) was mixed with macrophage lysate at various mixing ratios (usually 3 ratios, to reduce the chance that no ions were generated merely because of an analyte-matrix-ratio mismatch), and spotted in the dried droplet technique.

Additionally, while evaluating new lysing techniques, an already evaluated method was carried out side-by-side on an aliquot of the analyzed sample solution in order to have a direct reference, so that biological variation in the cultured macrophages, or instrument performance would not interfere with the evaluation process. Further, the cell count of each sample solution was taken into account with respect to solvent volumes, if possible, when the lysate solutions were constituted.

Table 2.3: Overview of macrophage lysing methods (in chronological order from top to bottom)

Method	Analyte	Lysing technique	Lysate preparation
Mechanical lysis (manual)	non-polarized NR8383 (pelleted at 2000rpm (=250xg) for 10min)	Triturated (ground with pestle) in 200 $\mu$ L 0.01% (w/v) O $\beta$ G	centrifuged at 13500rpm (=12,225xg) for 10min to sediment cell debris
Mechanical lysis (automated)	polarized NR8383 (pelleted at 2000rpm (=250xg) for 10min)	Bullet blender® (Next>>>Advance) in 10 $\mu$ L 0.01% or 0.1% (w/v) O $\beta$ G with ZrO <sub>2</sub> beads	centrifuged initially at 13500rpm (=12,225xg) then at 10000rpm (=9056xg) for 10min to sediment cell debris
Freeze-thaw	non-polarized NR8383 (pelleted at 2000rpm (=250xg) for 10min)	Freeze-Thaw (frozen at -20°C, stored for 3 days) in 100 $\mu$ L H <sub>2</sub> O defrosted in lukewarm water (3min)	10000rpm (=9056xg) for 10min
Ultra-sonication	non-polarized NR8383 (pelleted at 1100rpm (=138xg) for 10min)	Ultrasonic bath for 20min (cells in 40 $\mu$ L 0.1% (w/v) O $\beta$ G)	10000rpm (=9056xg) for 10min
Freeze-thaw (modified)	non-polarized NR8383 (pelleted at 1100rpm (=138xg) for 10min)	Snap-frozen (liquid N <sub>2</sub> ) in 40 $\mu$ L FT lysing buffer or 0.1% (w/v) O $\beta$ G 3x freeze-thaw cycles (defrosted on ice)	10000rpm (=9056xg) for 10min
Lyophilization	polarized NR8383 (pelleted at 1100rpm (=138xg) for 10min)	Snap-frozen (liquid N <sub>2</sub> ) (just the cell pellet) lyophilized for ~20h (pressure <50mbar)	Re-suspension in solvent (mostly H <sub>2</sub> O) optional trituration sedimentation of cell debris by centrifugation

n-octyl  $\beta$ -glucopyranoside (O $\beta$ G), 2,5-Dihydroxy benzoic acid (2,5-DHB), Methanol (MeOH), trifluoro acetic acid (TFA)

### 2.1.6. Optional desalting of macrophage lysate

The performance of matrices are generally regarded as quite sensitive to nonvolatile salts, which effectively prevent the ionization of analytes during the MALDI process.<sup>37</sup> To probe for detrimental concentration of salts (remainder from culture media, as well as originating from cytoplasm released during cell lysis) were present and inhibited ion signals, macrophage lysate was additionally desalted by the use of ZipTip® pipette tips and investigated with 2,5-dihydroxy benzoic acid. Essentially, a ZipTip® is a pipette tip that has a bed of chromatography media actin as the stationary phase incorporated in the tip, C18 in the evaluated case, to adsorb/partition analyte during the loading step, retain it during washing steps, and should release it in the elution step (due to appropriate solvent strength) (see *Table 2.4*). In this manner, it ideally concentrates and purifies targeted analyte.

*Table 2.4: Employed ZipTip® (OMIX, 96 C18, 100 µL) desalting protocol*

<b>Solvent/solution</b>	<b>Up&amp;Down pipetting (number of repetitions)</b>	<b>Purpose</b>
100 µL 0.1% TFA in acetonitrile	20	Pre-conditioning of ZipTip®
100 µL 0.1% TFA in water	20	
Sample solution	30	Loading of ZipTip®
100 µL 0.1% TFA in water	40	Washing step; replaced washing solution after every 10 repetitions
20 µL 0.1% TFA in 60% acetonitrile	35	Elution/concentration of retained sample

To check the retaining capability of the stationary phase, and for possible mass discrimination effects, the solution that was used to load the tip was analyzed by MALDI as well.

### 2.1.7. MALDI-TOF MS system and settings for analysis of mass spectra

The majority of the presented MALDI work on the activated macrophages was carried out on a Bruker Reflex III time-of-flight (ToF) instrument (Bruker Daltonics) equipped with a Nitrogen



laser (VSL-337 ND, LSI Laser Science, Inc), operating at 337 nm wavelength and laser shot frequency of 10 Hz. The mass spectrometer was used in positive ion mode, and both available configurations were investigated for their respective benefits: the linear mode, which permits a lower limit of detection, and the reflectron mode, in which an electrical ion mirror is used to compensate for a spread in the kinetic starting energies of the ions generated in the plume, and therefore allows for a higher resolution of the ion packages arriving at the detector. The ions were typically accelerated by the application of 26.5 kV (25 kV in reflectron mode) and focused by a potential of 14 kV applied to a focus lens. For the reflectron mode, the ion packages were deflected onto the detector by a potential of 26 kV applied to the ion mirror. Initially, methods were optimized to record spectra in reflectron mode (900 – 8000  $m/z$ ), and for the linear mode in the range of 2000 – 20000  $m/z$ . The external calibration of the instrument was performed using a solution of peptide calibration standard II (Bruker Daltonics Inc., Billerica, MA, USA) containing Bradykinin fragment 1-7, angiotensin II, angiotensin I, , substance P, bombesin, Renin substrate, ACTH clip 1-17, ACTH clip 19-39, and Somastostatin 28 and 1 mol/L 2,5-DHB matrix solution {[M+H]<sup>+</sup>: 757.4, 1046.5, 1296.7, 1347.7, 1619.8, 1758.9, 2093.1, 2465.2, and 3147.5} for the reflectron mode, or protein calibration standard I (Bruker Daltonics Inc., Billerica, MA, USA) containing Insulin, Ubiquitin I, Cytochrom C, Myoglobin with 1 mol/L CHCA matrix solution {[M+H]<sup>+</sup>: 5734.51, 8565.76, 12360.97, 16952.30 [M+2H]<sup>2+</sup>: 6180.99, 8476.65} for the linear mode.

The mass spectra were analyzed with FlexAnalysis 3.3 software (Bruker Daltonics). For spectra recorded in the linear mode, typically the baseline was subtracted (TopHat algorithm) and a SavitzkyGolay filter (10  $m/z$  width, 2 cycles) was applied to smooth the spectra to aid in peak picking (centroid mode, 20 Da width at 80% height, signal-to-noise threshold of 100). For

spectra obtained in reflectron mode, the baseline was subtracted (TopHat algorithm) and the SavitzkyGolay filter (0.5  $m/z$  width, 1 cycle) was applied to smooth the spectra to aid in automatic peak picking (centroid mode, 1 Da width at 80% height, signal-to-noise threshold of 6). The intensity of all presented MALDI spectra is normalized in a way that the most intense peak is considered 100%, and the remaining peaks are relative to it in their depicted size. This is to emphasize the relevance of the exhibited fingerprint, and not the absolute signal intensity, which would be generally given in instrument-specific arbitrary units. It should further be noted that the shift of observed  $m/z$  in the mass spectra is mainly due to a combination of the difference in sample morphology (i.e. the thickness of the prepared matrix co-crystals, the following difference in distance of the generated ions to the acceleration electrode, and the resulting differential amount of absorbed kinetic energy upon acceleration) and the lacking ability to efficiently compensate for this in the linear ToF mode of the employed, dated instrument. A shift of the observed  $m/z$  by +/- 10 Da across the MALDI spectra generated in the linear mode was accepted as long as this trend was consistent within the spectrum.

## 2.2. Results and discussion

### 2.2.1. Impact of matrix selection on observed mass spectra

With the exception of 1,5-diaminonaphthalene (1,5-DAN), all investigated matrices (*Table 2.2*) yielded spectra of the macrophage lysate in the investigated range of 2000-20000  $m/z$  (see *Figure 2.1*). 2,5-dihydroxybenzoic acid (2,5-DHB) prepared in 90% methanol with 0.1% TFA was under the investigated conditions the most reproducible matrix with respect to observed unique ions, and relative ion intensities. 3,5-dimethoxy-4-hydroxy cinnamic acid (“sinapinic acid” SA) resulted in equally information-dense spectra. In the case of SA, only the dried droplet preparation was initially employed, which exhibited a relative high fluctuation in observed

relative ion signal strength (see comparison of 2,5-DHB vs SA, *Figure 2.2*), which lead to the preferential use of 2,5-DHB. At a later stage, though, the layer preparation of SA was tested, and found to be of advantage based on the identical amount of observed ions (when compared to 2,5-DHB), but increased homogeneity of the applied sample.<sup>73</sup> *Figure 2.3* depicts spectra recorded in the reflectron mode (top), and the linear mode (bottom) of macrophage lysate spotted in the dried droplet method with an equal volume of 2,5-DHB dissolved in 90% methanol/0.1% TFA. The inset shows the most conserved fingerprint region of the sample in the range of 3900 – 6500 Da  $m/z$  in an overlay of the reflectron and the linear mode. This display further demonstrates the enhanced peak resolution of the reflectron mode compared to the linear mode, which was used to investigate potential unresolved, unique ion signals. This fingerprint, especially the most intense peak around 4960 Da, was observed with every tested matrix (with the exception of 1,5-DAN) with differing relative intensities of the observed peaks. This prominent peak was found to be thymosin beta-4, an actin-binding peptide, typically abundantly present and characteristic for monocytes/macrophages, by Kannan et al. in chicken macrophage.<sup>79</sup>

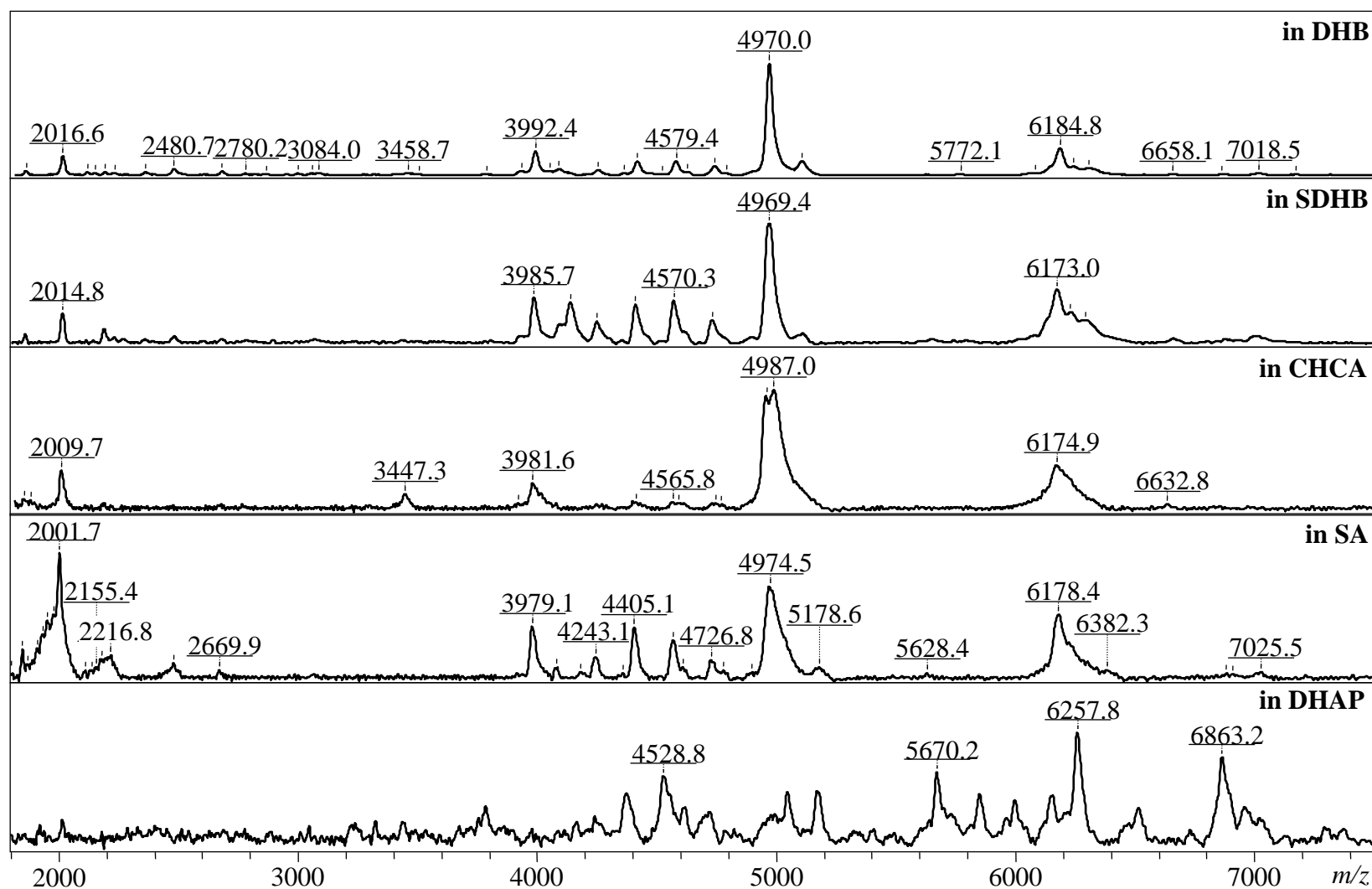


Figure 2.1: Overview of mass spectra produced from macrophage lysate spotted with matrices according to Table 2.2. From top to bottom: in 2,5-DHB, “super” DHB, CHCA, SA (dried droplet preparation), and DHAP. The spectra were analyzed as described in 12.1.7. , so only signals with  $S/N > 100$  are labeled (with  $m/z$ , or with tick marks), and in this way serve as indicator for spectra quality.

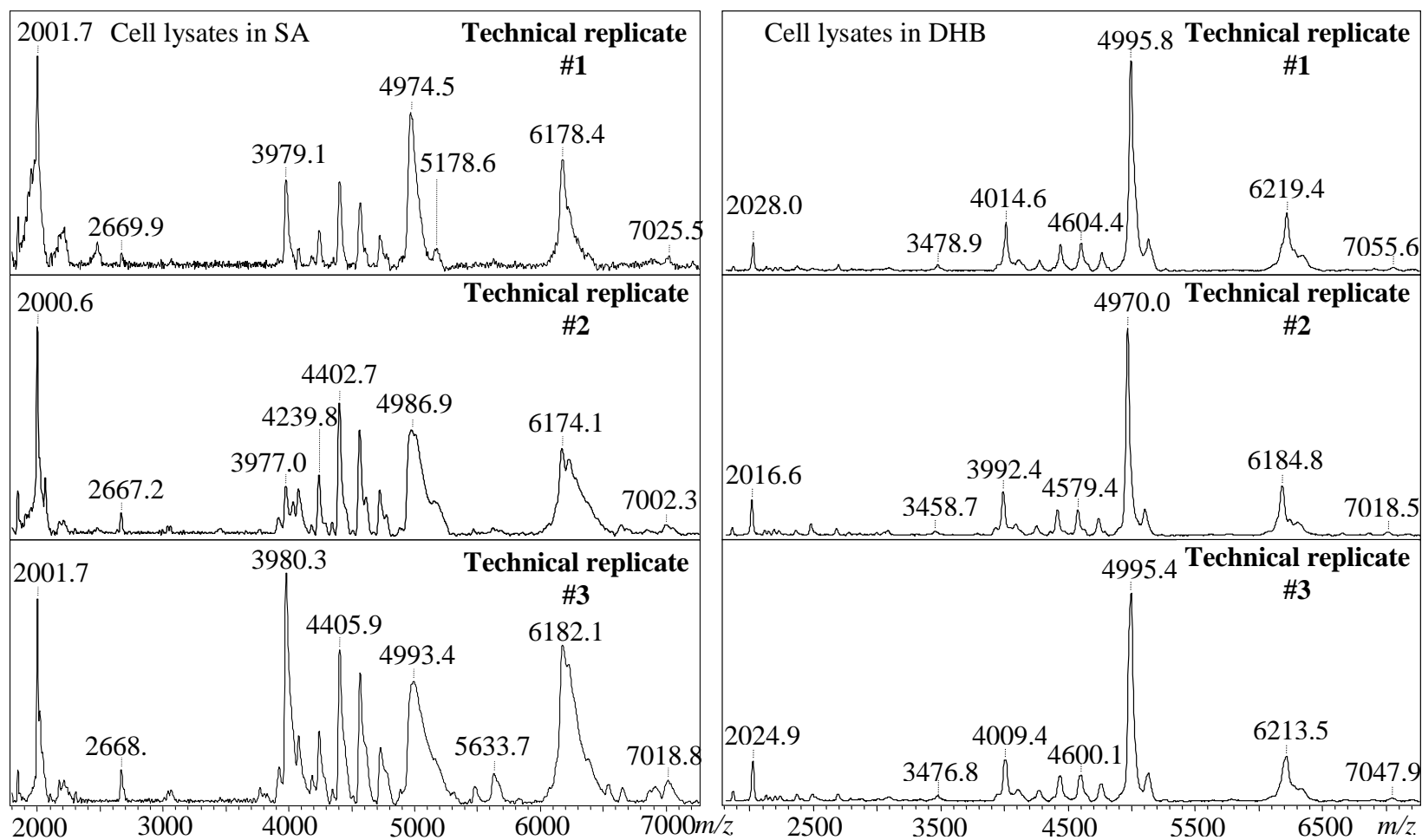


Figure 2.2: Comparison of reproducibility of cell lysate spotted with sinapinic acid (SA, dried droplet preparation, left), and with 2,5-dihydroxy benzoic acid (2,5-DHB, right). Both sides represent technical replicates prepared with the same sample.

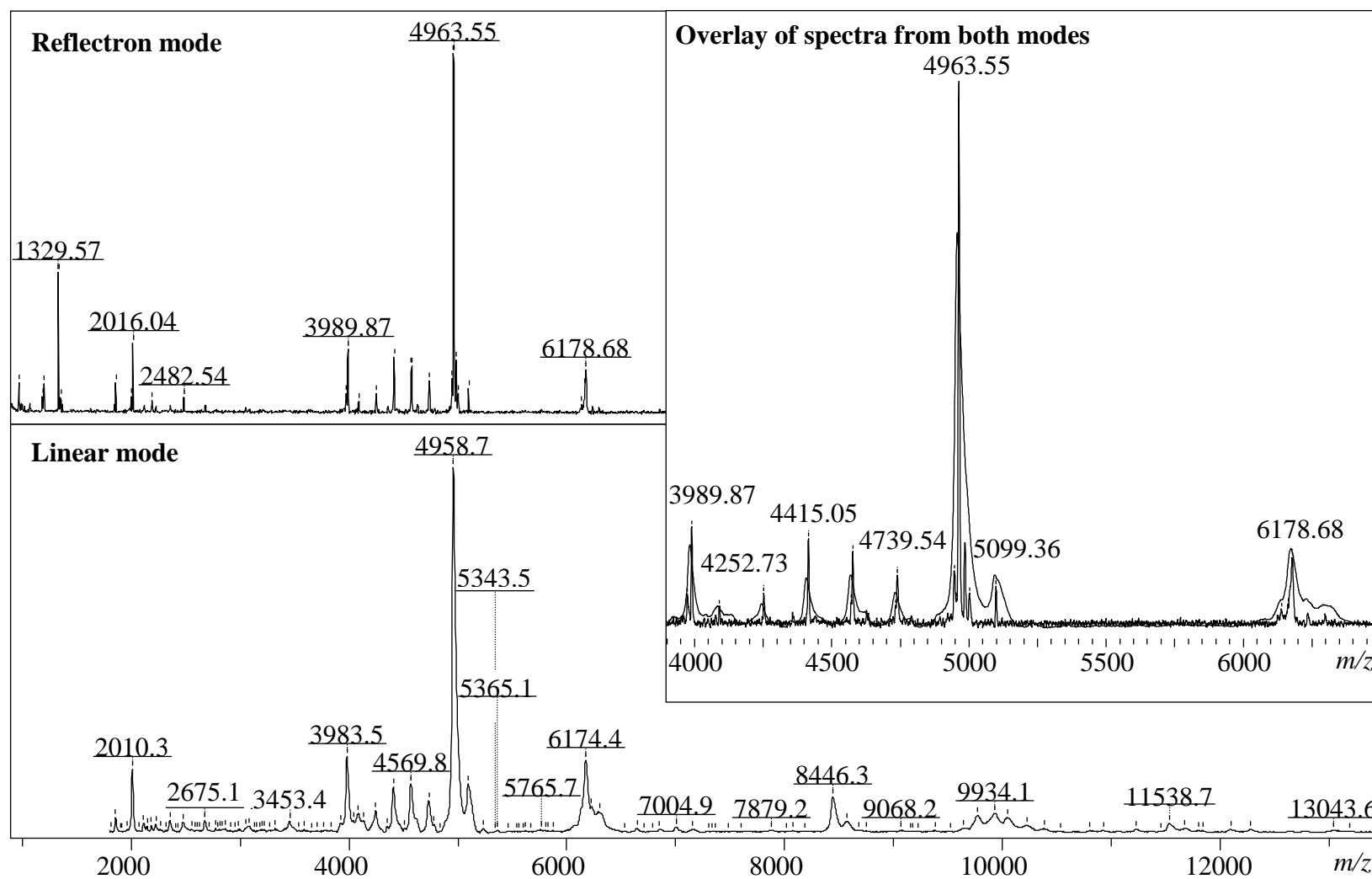


Figure 2.3: Mass spectra of macrophage lysate (NR8383 cells) spotted with 2,5-dihydroxy benzoic acid (1M in 90% methanol, 0.1% trifluoroacetic acid). Spectra recorded in reflectron mode and displayed in the  $m/z$  mass range of 900 – 7000 Da (top), and spectra recorded in the linear mode with the  $m/z$  range of 1900 – 135000 Da displayed (bottom). The inset depicts an overlay of both modes to demonstrate difference in obtained peak resolution, and to show the preserved fingerprint region, 3900 – 7000 Da, of the NR8383 macrophages.

### 2.2.2. 2,5-DHB: Macrophage cell dilution experiment and desalting effect

Investigating the performance of the matrix 2,5-DHB further, the required minimum amount of macrophage cells to obtain similar fingerprints as depicted in *Figure 2.3* was explored, as well as the impact of nonvolatile salt.

In a dilution experiment, in which macrophage lysate was diluted and prepared at decreasing concentrations with 2,5-DHB (1M, dissolved in 90% methanol, 0.1% TFA, dried droplet) it could be observed that, by the calculated dilution factor, lysate corresponding to approximately 900 macrophages would suffice to produce the observed fingerprint (*Figure 2.4*). However, this number can be seen as upper limit, since this experiment was carried out with the initial lysing technique that could be optimized in later experiments (see below).

The application of the ZipTip® protocol did not improve the observed signal intensity or produce additional peaks. Instead, strong mass discrimination were observed (*Figure 2.5*). While the sample that was eluted as the purified product was enriched in signals representing ions up to  $\approx 1350$   $m/z$ , and depleted in signals representing higher  $m/z$  ions, the solution that was used in the loading step exhibit the opposite behavior. This indicates an analyte retention problem, which could possibly be alleviated through adjustments in the protocol (e.g. less concentrated loading solution, different solvent systems for washing/eluting, general variation in step order/repetition). However, it does not seem necessary to desalt the sample, since 2,5-DHB seems tolerant enough for the trace levels of salt in the analyte solution, so the additional step of desalting was omitted in the work-up protocol, as it would also be impracticable to apply to tissue sections.

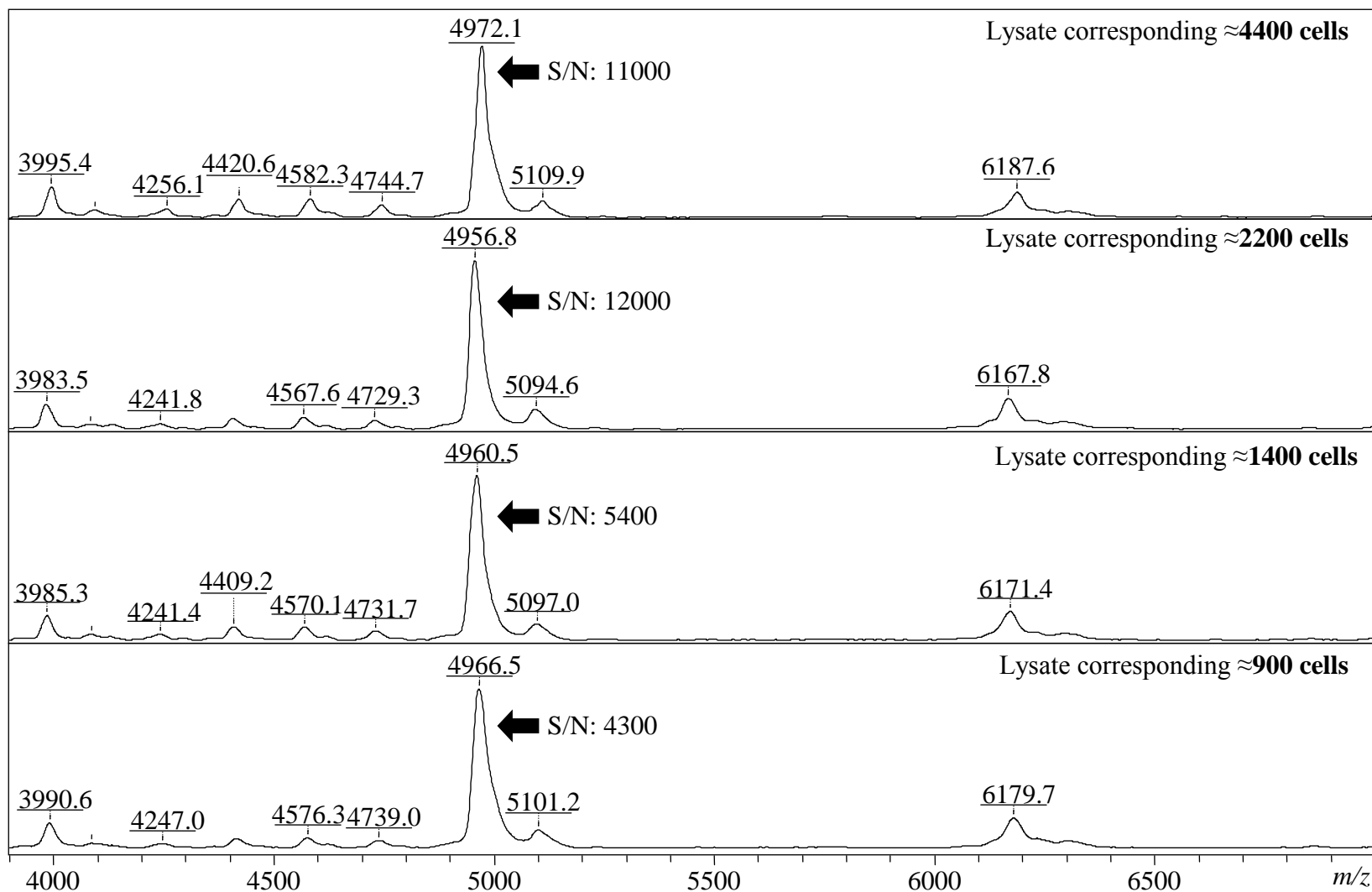


Figure 2.4: Amount of macrophage cells needed to produce typical mass spectral fingerprint. Lysate was produced by initial mechanical lysis protocol (trituration), and the resulting lysate was spotted with 2,5-DHB (1M in 90% methanol/0.1% TFA, dried droplet). The lysate was produced from  $2.6 \times 10^6$  quiescent macrophage cells, and diluted accordingly so that lysate of  $\approx 4400$  cells (top), lysate of  $\approx 2200$  cells (2nd), lysate of  $\approx 1400$  cells (3rd), and lysate of  $\approx 900$  cells (bottom) were applied per dried droplet preparation. The arrow indicates the S/N of the most intense peak in each spectrum.



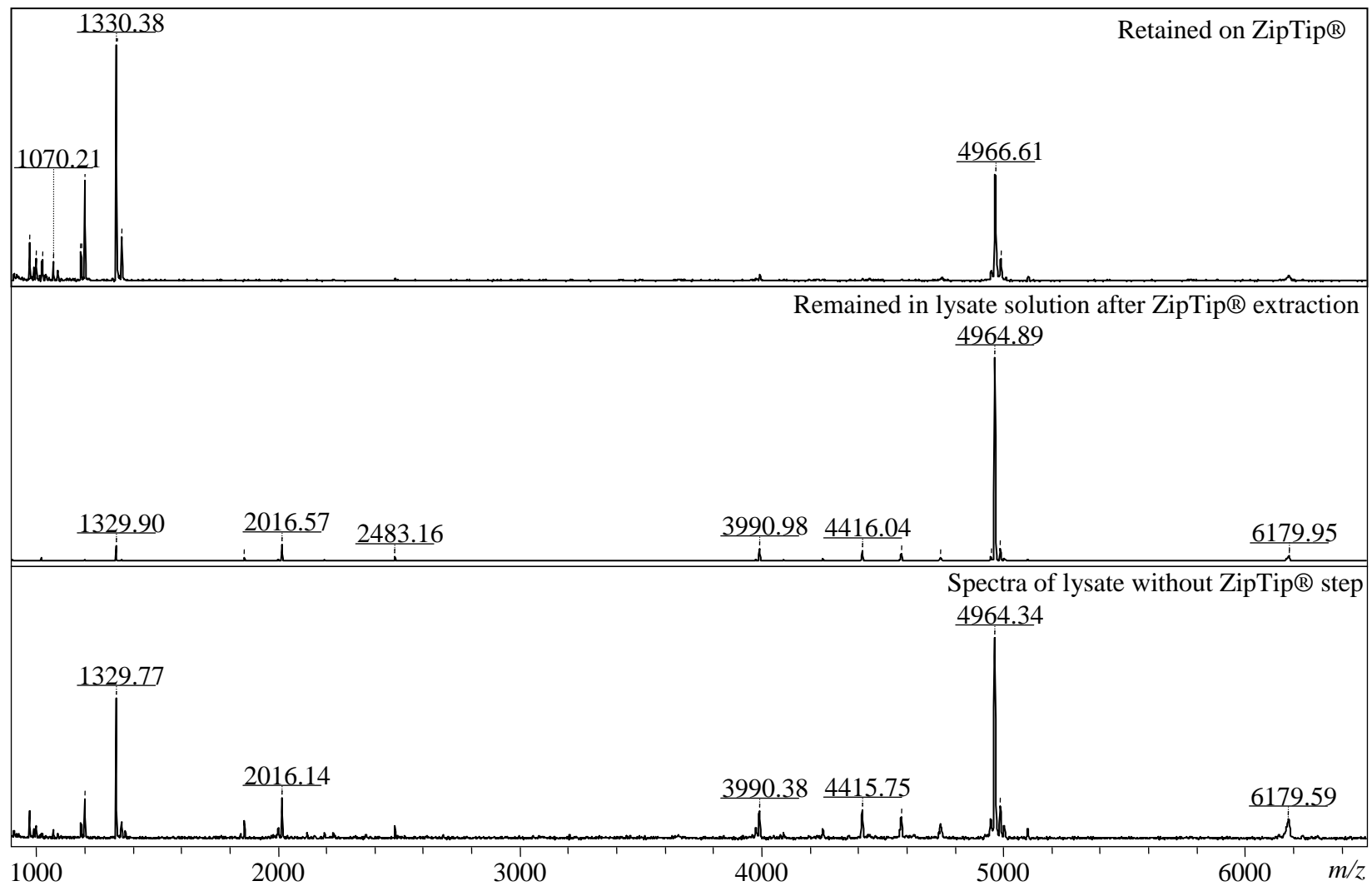


Figure 2.5: Result of ZipTip® extraction/desalting. Purified macrophage lysate (top), analyte remaining in the extracted lysate (middle), and reference spectra of lysate without ZipTip® extraction.

### 2.2.3. Effect of extraction solvent and acidity

Surprisingly, all but acetonitrile/0.1% TFA, which did not produce any signal at all, of tested solvent systems (*Table 2.1*) produced mass spectra (see *Figure 2.6*) exhibiting the dominant fingerprint region in between 3900 – 6500 Da  $m/z$ , with only minor variation of unique, low intense peaks in the remaining  $m/z$  range. This result could indicate that the ions representing this fingerprint region are very efficiently ionized, and hence scavenge most of charges present in the MALDI plume,<sup>84</sup> almost independently of how well they are extracted based on their respective hydrophobicity. In contrast, extracting the macrophages with 2.1 % (v/v) TFA drastically changed the observed mass spectra (*Figure 2.7*) compared to *Figure 2.3*. Approximately two times more unique ions could be observed within the range of 1500 – 6000  $m/z$ , while, at the same time, the observed relative signal intensity of the fingerprint region seemed to become less reproducible. A close investigation of this phenomenon, however, revealed that the obtained spectra are not reproducible, exhibiting differing unique ions almost each repeated experiment. This may indicate that molecules of higher mass, especially proteins, could be randomly hydrolyzed to produce fragments of very unsteady nature, which excludes the approach of increasing the content of TFA to 2.1 % (v/v) in the preparation protocol.

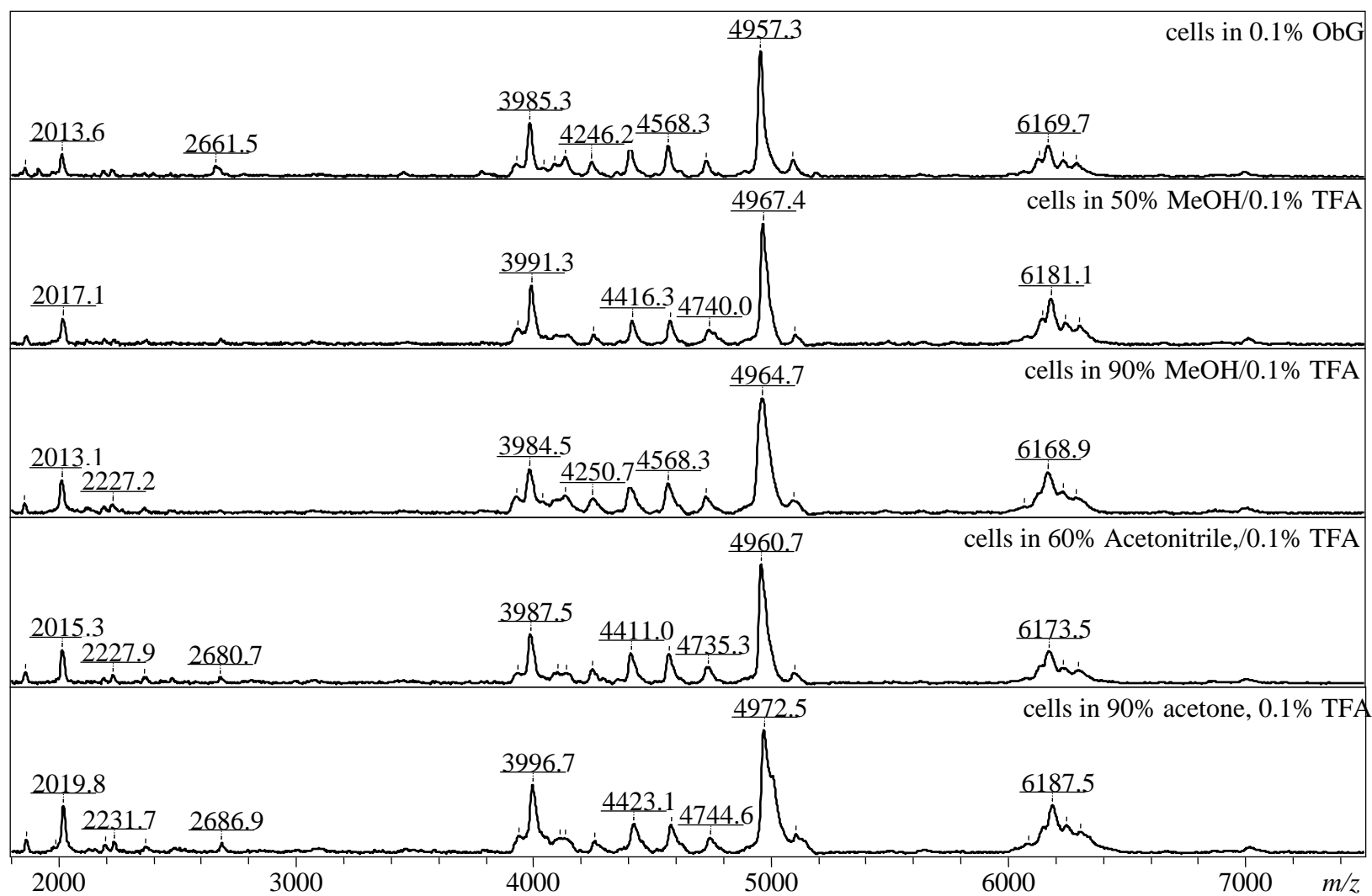


Figure 2.6: Mass spectra of macrophage cell pellets extracted with differing solvent systems, but producing almost identical mass spectral fingerprint. Extractions solvents were 0.1% *n*-octyl  $\beta$ -glucopyranoside (ObG) (top), 50% methanol/0.1% TFA (2nd), 90% methanol/0.1% TFA (3rd), 60% acetonitrile/0.1% TFA (4th), and 90% acetone/0.1% TFA (bottom). All extracts were spotted in dried droplet with 2,5-DHB from 90% methanol/0.1% TFA

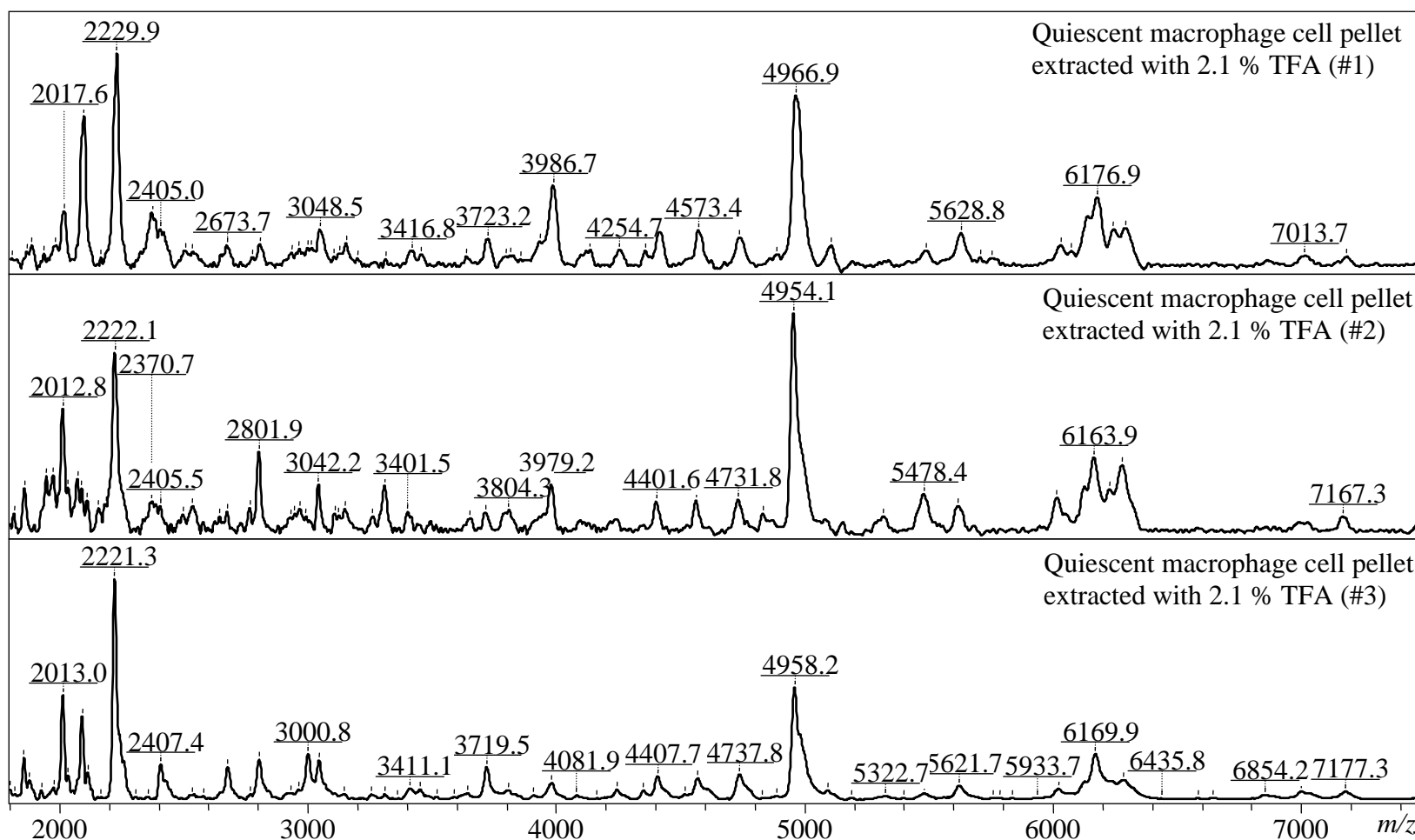


Figure 2.7: Mass spectra of macrophage cell pellets extracted with 2.1% TFA, and spotted in dried droplet with 2,5-DHB from 90% methanol/0.1% TFA. Each spectra represents an individual extraction. It is noticeable that about 2 times more unique peaks (in contrast to Figure 2.3) are present, but the comparison of the independently extracted cell pellets exhibits the lack of reproducibility of these extra peaks.

#### 2.2.4. Impact of lysing method on observed mass spectra

*Figure 2.8* shows a comparison of spectra obtained from macrophages subjected to three different lysing techniques involving the bullet blender, freeze thaw lysis, and the sonication approach (see *Table 2.3*). All samples were prepared from approximately  $2 \times 10^5$  quiescent macrophages and were spotted in the dried droplet technique with an equal volume of 2,5-DHB dissolved in 90% methanol, 0.1% TFA. It can be noted that the observed fingerprint is independent of the employed lysing method. However, the sonication approach was found to provide the most intense signal based on the observation that sample spots could be probed longer, and at different spots, for more overall signal.

Ultimately, the lyophilization approach was accepted as standard. It provided comparatively strong signal as the sonication approach, but would also inhibit sample degradation by removal of solvent, provide a long shelf life (lyophilized samples would exhibit identical LC-MS spectra even after storage for >2 months at  $-20^\circ$ ), and would be compatible with future tissue section preparation.

#### 2.2.5. Mass spectra of differing activation states in 2,5-DHB

*Figure 2.9* depicts representative mass spectra of macrophage lysate of quiescent, LPS-activated, and IL-4 activated macrophages prepared with 2,5-DHB (1 M in 90% MeOH / 0.1% TFA) in dried droplet technique. Lysates of eight independent activation experiments (for each activation state, and control macrophages) were analyzed (three technical replicates of each sample), but no reproducible mass spectral fingerprint was found that would allow identification of activation state.

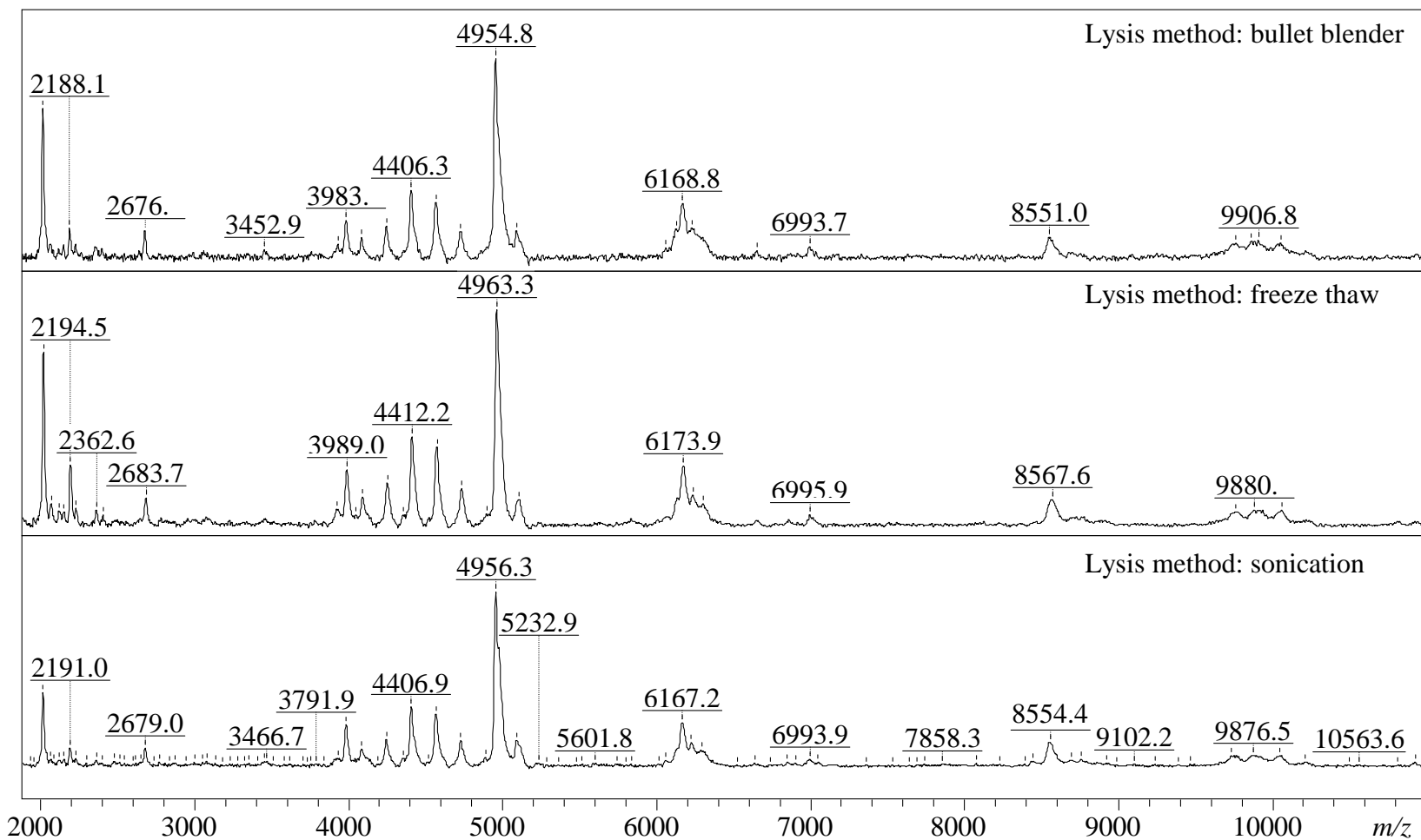


Figure 2.8: Overview of three differing lysing techniques: bullet blender (top), freeze thaw (middle), and sonication (bottom). The lysate produced with each technique was spotted with 2,5-DHB in 90% methanol/0.1% TFA, and the obtained spectra exhibit an identical mass spectral fingerprint.

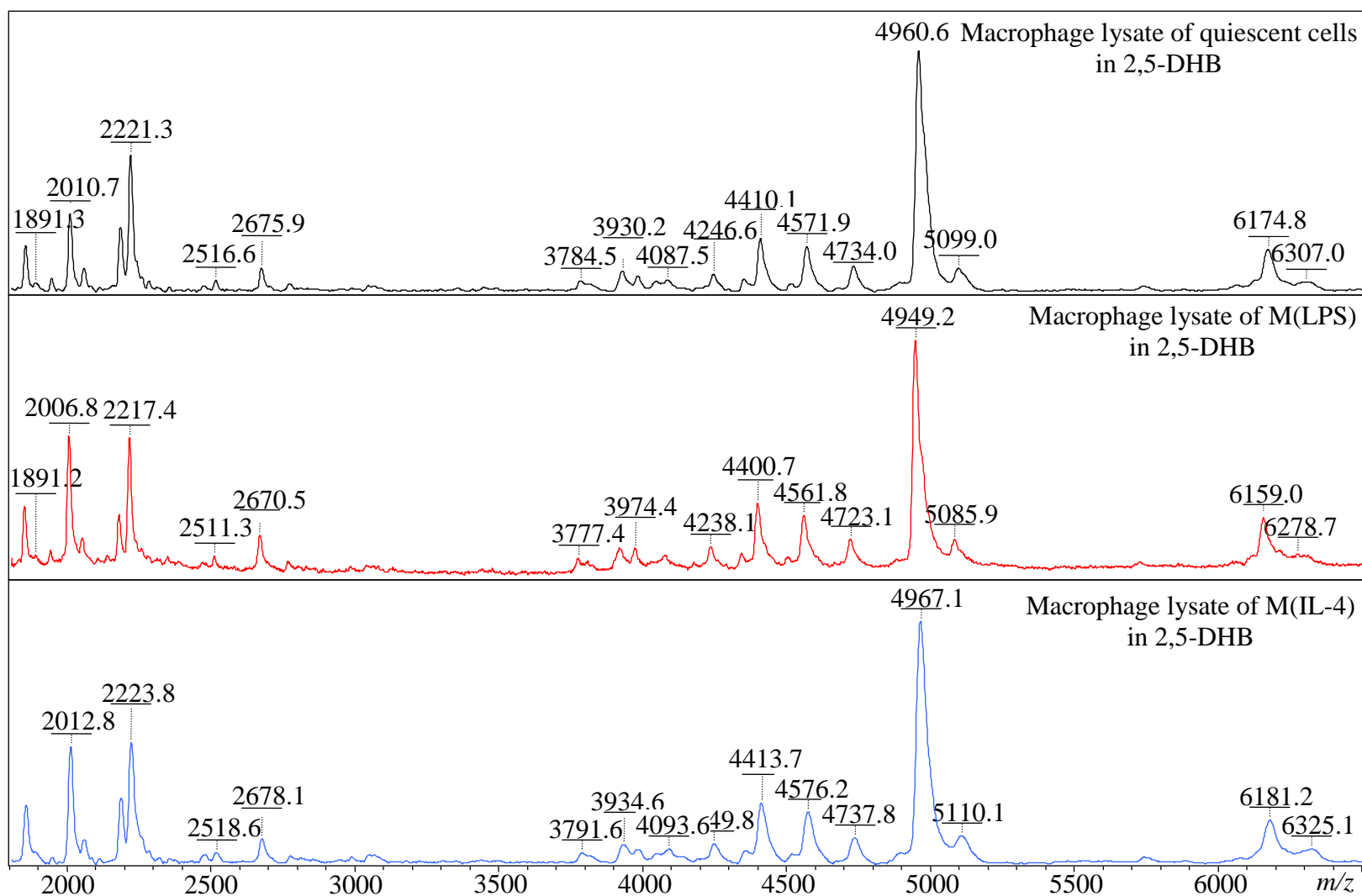


Figure 2.9: Representative mass spectra of macrophage lysate of quiescent (top), LPS-activated (middle), and IL-4 activated (bottom) cells prepared with 2,5-DHB (1 M in 90% MeOH / 0.1% TFA) in dried droplet technique. All mass spectral fingerprint appear indistinguishable from each other.

### 2.3. Need for separation – transition to LC-MS

Although the mechanism of MALDI has been subject of extensive research for the past 30 years, the desorption/ablation and the ionization process are still poorly understood. No unifying model for analyte ion formation could be established so far, but both currently proposed models consider charge transfer between the gas phase ions/molecules in the plume following the laser irradiation a central mechanism of charge distribution.<sup>55</sup> This dynamic process, however, is influenced by numerous parameters,<sup>56</sup> so the essential aspect, the reproducibility of observed ion signal from complex mixtures, in the mass spectral fingerprint approach (as described in 1.5. ) is of pure experimental nature.

In the case of the macrophage lysate, the mass spectral fingerprint, especially in the range of 4000 – 6500  $m/z$  (compare inset *Figure 2.3*), appears to be well conserved across differing activation states (*Figure 2.9*), differing extraction solvents (*Figure 2.6*), and, to a certain degree, across different employed matrices (*Figure 2.1*). This could indicate the dominant and relative strong ionizability of the corresponding molecules, and the concomitant suppression of other ion signals that could potentially differentiate the activation states. To test this hypothesis, the next chapter presents experiments on the separation of the complex mixture with the help of high-performance liquid chromatography, and resulting mass spectra of the eluting sample of lower complexity.



### Chapter 3: HPLC-MS of *in vitro* activated macrophages

The transition to a protocol involving the separation step of liquid chromatography, and the subsequent mass spectrometric analysis of the dissolved analyte through an electrospray (ESI) source made it necessary to reconsider the MALDI MSI approach. Fortunately, liquid extraction based methods for the analysis of tissue sections have been proposed as alternatives,<sup>85-87</sup> and automated, semi-continuous techniques were demonstrated to be compatible with HPLC.<sup>88-90</sup>

#### 3.1. Experimental section

##### 3.1.1. Chemicals and equipment

In addition to the chemicals and equipment used in chapter 2: ultra-pure water was obtained through filtering (Milli-Q purified, resistivity of 18 M $\Omega$  per cm, Millipore Corporation, Billerica, MA, USA). Microsampling vials, 0.25 mL C/T PP, and the appropriate caps, 11mm orange snap PTFE/Sil, for the LC-autosampler were obtained from Sun-Sri (Rockwood, TN, USA). The desalting/concentration tip (NuTip® C18, 10  $\mu$ L) were obtained from Glygen Corporation (Columbia, MD, USA).

Additional used equipment includes the HPLC-MS system consisting of Hewlett Packard 1100 liquid chromatography (now Agilent Technologies, Santa Clara, CA, USA), with the Discovery BIO wide pore C18 column (15 cm x 4.6 mm, 5  $\mu$ m, obtained from Sigma-Aldrich (St. Louis, MO, USA)) and the internal variable wavelength detector (G1314A) with a deuterium lamp (G1314-60100), and a semi-micro flow cell (G1315-60011, 6 mm path length, 5  $\mu$ L volume) installed. The hyphenated mass spectrometer was an Esquire ion trap (Bruker Daltonics, Billerica, MA, USA), and a fraction collector Model 2128 (Bio-Rad Laboratories, Hercules, CA, USA) for the alternative setup. Additionally, the Ultraflex extreme (Bruker Daltonics Billerica, MA, USA) was used for MALDI ToF/ToF experiments. For sample preparation, the bench-top

centrifuge VWR minifuge (VWR, Radnor, PA, USA), and the vacuum centrifuge CentriVap DNA Centrifugal Concentrator (Labconco, Kansas City, MO, USA) were used.

### 3.1.2. Preparation of macrophage lysate extract

Macrophages were cultured and activated as described in chapter 2 (see 2.1.4. For reasons described above (2.2.4. ), the harvested cell pellets of approximately  $1-1.5 \times 10^6$  macrophages each were lyophilized in a 1.5 mL Eppendorf tube to yield dry, powdered sample.

Each sample was extracted by re-suspending the powdered macrophages in 100  $\mu$ L of HPLC-grade water through up and down pipetting, followed by brief, vigorous vortexing to form a slightly cloudy suspension. The solution was then centrifuged at 2000 g for 2 min to sediment out the floating matter. After repeating this vortexing and centrifuging step once, 90  $\mu$ L of the supernatant was carefully removed with a pipette, and transferred to a 250  $\mu$ L sample vial. All prepared extracts were immediately analyzed by LC-MS to minimize any potential degradation.

### 3.1.3. LC-MS – Settings and evaluation of system

The liquid chromatograph was set up to run in binary gradient elution (*Table 3.1*) with 0.1 % (v/v) formic acid in ultra-pure water as running solution A, and acetonitrile with 0.1 % (v/v) formic acid as organic phase, B. Typically, 30  $\mu$ L of sample was injected through the autosampler, and the sample was separated at a flow rate of 0.5 mL per minute through the reverse phase C18 wide pore column with a 30 min gradient elution. The eluting compounds were either directed into the Esquire ion trap through the electrospray interface, or the eluting solution was collected by the fraction collector (see below, 3.1.5. ).

In the case of direct infusion into the mass spectrometer, 4.2 kV were applied to the electrospray needle, the solution was nebulized at 32 Psi ( $N_2$ ), and the solvent evaporation was

enhanced by heated (300 °C) N<sub>2</sub> sheath gas at a flow rate of 12 L per minute. The mass range was set to 375 – 2000 Da *m/z*, the ion polarity was set to positive, the ion charge control (ICC) to 50000, and the ion scan rate to 2000 Da per second (lowest limit-of-detection, regular resolution).

To evaluate signal stability of the LC-MS system, 30 µL aliquots (n = 3) of macrophage lysate (extract from quiescent, and one from LPS-activated macrophages) were analyzed consecutively (remaining lysate was stored in the fridge for the duration of each LC-MS run), and the resulting spectra were analyzed as described below (3.1.6. ). Using actual lysate imposed the constraint of limited sample volume (100 µL), but was deemed necessary to evaluate the system stability under experimental conditions.

#### 3.1.4. Development of HPLC elution protocol

In liquid chromatography, the analytes continuously partition between the stationary phase (hydrophobic in the present case of the employed reversed-phase column), and the mobile phase (relative hydrophilic due to the share of H<sub>2</sub>O in the running buffer).<sup>35</sup> If other factors influencing this partitioning like temperature, or column material are kept constant, the time it takes for the molecules to traverse the column, i.e. the retention time, is a function of elution volume and solvent composition. In the case of polypeptides, however, a “hydrophobic foot” can be the result of sequences of hydrophobic amino acids, which then adsorbs to the hydrophobic column material, resulting in complete retention. These molecules can only desorb and elute if a specific number of organic modifiers, called ‘Z’ by Geng and Regnier,<sup>91</sup> is reached. This desorption is complete and instant once the very narrow concentration window of the organic modifier is reached.<sup>92</sup> Based on this, and on further considerations by Carr,<sup>92</sup> the elution protocol was

developed from a simple gradient elution (ramping from 2 % to 100 % acetonitrile within 30 min), to the stepwise protocol in *Table 3.1*.

*Table 3.1: HPLC-gradient elution protocol*

<b>Time range [min]</b>	<b>Increase in acetonitrile-%</b>	<b>Change rate [% per min]</b>	<b>Comment</b>
0 – 25	12 – 40	1.12	investigated range
25 – 30	40 – 95	11	cleaning step to avoid carry-over
30 – 35	95 (constant)	-	
35 – 40	12 (constant)	-	equilibration of column for next injection

Used for separation of macrophage extract with Discovery BIO wide pore (C18) column

### 3.1.5. Preparation of collected fractions for MALDI

In the alternate set up, where the HPLC was attached to the fraction collector, samples of 1 min intervals were collected in 1.5 mL Eppendorf tubes. To confirm that the injected sample was producing a similar LC-MS fingerprint in this situation, a regular LC-MS run on an aliquot of a macrophage lysate was always performed right before fractions were collected, and, additionally, the UV trace recorded at 254 nm by the internal detector of the HPLC was compared of both successive runs to confirm correct timing of collection. Following the collection, fractions were loaded without delay into the centrifugal concentrator to evaporate the solvent to dryness under reduced pressure (< 20 mbar) and at elevated temperature (60 °C). Depending on the number of simultaneously dried fractions, this took 2 to 6 hours.

The resulting residues were re-suspended by adding 7 µL of 15% acetonitrile/0.1% TFA (half saturated with SA) to each dried fraction, followed by brief, vigorous vortexing to visibly cover the inside walls of the respective Eppendorf tube. The liquid was collected at the bottom of the container by centrifuging for 30 sec at 2000 g. 1.5 µL of the resulting analyte/matrix solution was applied to a MALDI target pre-spotted with SA (*Table 2.2*, layer preparation) in technical triplicates.

### 3.1.6. Spectra processing, analysis and evaluation

LC-MS spectra were analyzed with DataAnalysis (version 4.0 SP 4 Build 281, Bruker Daltonics). The default display mode is total ion chromatogram (TIC), in which the sum of the signal intensities across the investigated  $m/z$  range of each recorded mass spectrum is plotted against the elution time. However, increasing the percentage of acetonitrile leads to a general enhancement of observed signal in ESI-MS with traditional columns (4.6 mm diameter),<sup>37</sup> which confounds the TIC by amplifying the chemical noise (see *Figure 3.1*), which was also documented by the column manufacturer (organic modifier was 0.1 % TFA in methanol in the described case).<sup>93</sup> To address this, LC-MS spectra were visualized by base peak extracted chromatograms (BPC), in which the most intense ion signal of each mass spectrum (integrated in the range of  $\pm 0.5$  Da) is plotted against the elution time. However, this display method was always validated by manually evaluating the mass spectra (apex peak finder with  $S/N > 10$  as criteria) obtained during each individual chromatogram, and observed differences in signal intensities were further explored by analyzing the corresponding mass spectrum for multiply charged ions. To quantify ion signals, all charge states belonging to a molecule (e.g. the annotated ion signals in *Figure 3.4*) were extracted (integrated  $\pm 0.5$  Da of peak) and summed up. This was displayed in extracted ion chromatogram (EIC) mode, and the resulting peaks in EIC were integrated for quantification purpose. To compensate for observed performance drift of ion signal intensities, as well as slight differences in extracted cell counts, the integrated ion signals of each run were normalized by the sum of all ion signals observed within the same experiment.<sup>94</sup> Thus, the spectra are transformed from an absolute to a relative intensity scale, allowing comparisons of molecular fingerprints obtained in the LC-MS experiments (an alternative normalization based on the most intense peak at minute 10 resulted in the same trend).

To evaluate the standard deviation in observed signal introduced by the LC-MS system, 30  $\mu\text{L}$  aliquots (three) of lysate from quiescent macrophages were consecutively analyzed (extract was prepared immediately before the initial run, and kept at  $-20^\circ$  in between injections). The EIC of 10 multiply charged ions were integrated and the average, weighted, relative standard deviation of these technical replicates was determined to evaluate reproducibility of the performance of the employed LC-MS system.

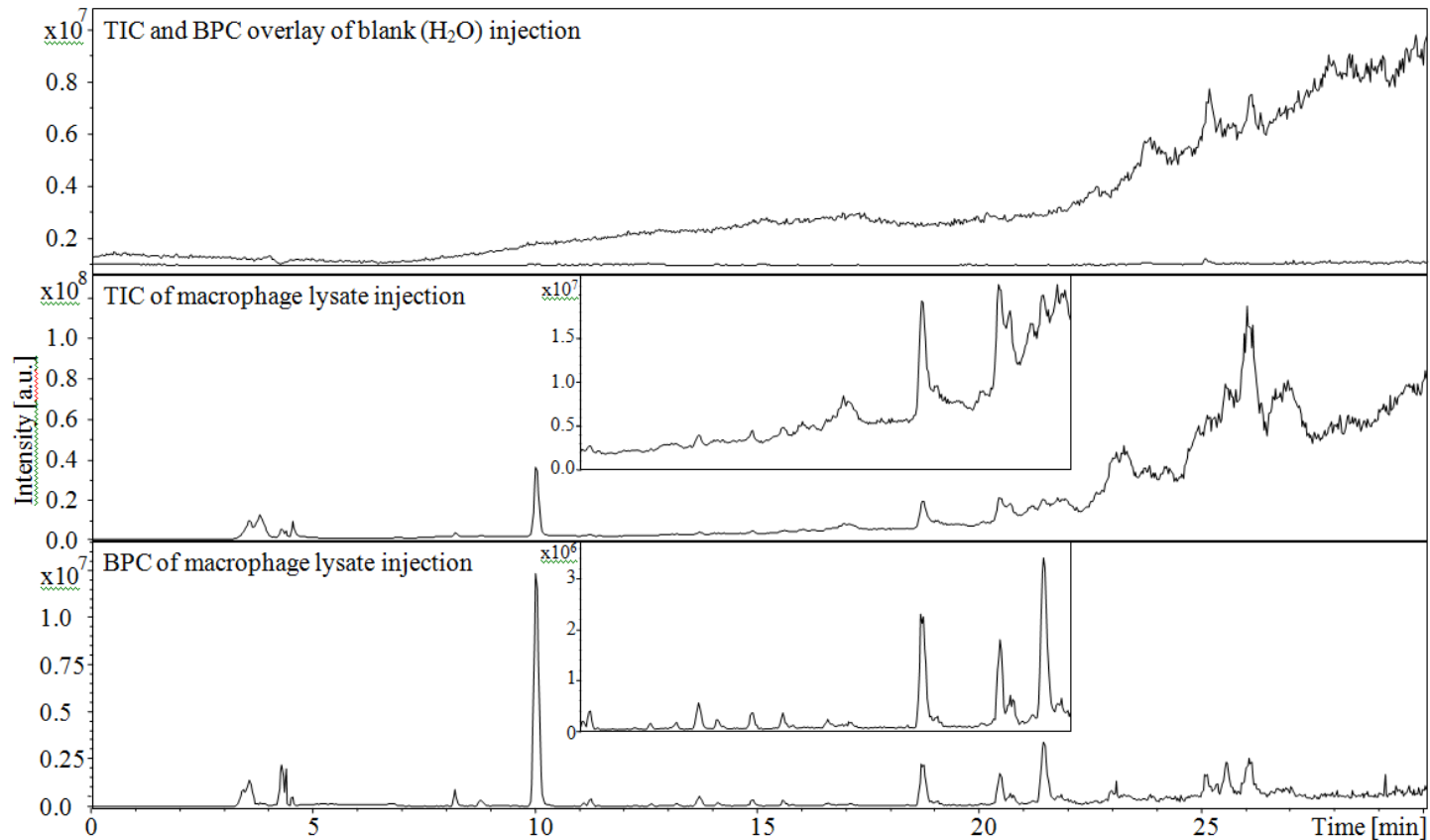


Figure 3.1: LC-MS chromatograms of experiments following the same gradient elution protocol (see Table 3.1) and displayed as total ion chromatogram (TIC, top and middle), and as base peak extracted chromatogram (BPC, top and bottom). The top chromatogram is an overlay of the TIC (rising line) and the corresponding BPC (flat line). This TIC (water injected as sample) demonstrates the raise of the baseline with the increase of acetonitrile in the elution buffer. The chromatograms depicted in the middle (TIC) and at the bottom (BPC) are differential display methods of the same raw data representing a typical LC-MS chromatogram obtained by injecting quiescent macrophage lysate. The insets display a magnified version (minute 11 to 22) of the respective chromatograms. Note: scale difference

### 3.1.7. Tryptic digestion of collected fractions containing the potential biomarker and preparation for MALDI experiment

After confirming (see *Figure 3.1*) that the potential biomarker would elute under the employed elution protocol (*Table 3.1*) after  $\approx 21.5$  min, four fractions (minutes 21-22, 22-23, 23-24, and 24-25) were collected. To increase the amount of sample for the digestion, a total of three lyophilized, quiescent macrophage cell pellets ( $\approx 1.5 \times 10^6$  macrophages each) were extracted with 100  $\mu\text{L}$  each (as described above in 3.1.2. ), and 75  $\mu\text{L}$  of each extract was injected for LC-fraction collection. The combined (each elution interval combined separately), dried fractions (as described above under 3.1.5. ), were each subjected to the in-solution digestion protocol<sup>95</sup> described in *Table 3.2*.

*Table 3.2: Digestion protocol employed to digest collected, dried LC fractions of quiescent macrophages*

<b>Description of step</b>	<b>Comment</b>
Re-suspension of dried fraction in a total volume of 100 $\mu\text{L}$ of 50 mM $\text{NH}_4\text{HCO}_3$	
<ul style="list-style-type: none"> <li>• Addition of 5 <math>\mu\text{L}</math> 200 mM dithiothreitol solution (prepared in 100 mM <math>\text{NH}_4\text{HCO}_3</math>)</li> <li>• Boil for 10 min on a hot water bath</li> <li>• Spin down (<math>\approx 10</math> s at 2000 g)</li> <li>• Incubation at room temperature for 1 h</li> </ul>	Reduction of any present disulfide bonds to form thiol (-S-H) groups.
<ul style="list-style-type: none"> <li>• Addition of 4 <math>\mu\text{L}</math> 1 M iodoacetamide (prepared in 100 mM <math>\text{NH}_4\text{HCO}_3</math>)</li> <li>• Brief vortexing, spin down (<math>\approx 10</math> s at 2000 g)</li> <li>• Incubation at room temperature for 1 h</li> </ul>	Alkylation of each present thiol to form a carbamidomethyl group
<ul style="list-style-type: none"> <li>• Addition of 20 <math>\mu\text{L}</math> 200 mM dithiothreitol solution (prepared in 100 mM <math>\text{NH}_4\text{HCO}_3</math>)</li> <li>• Brief vortexing, spin down (<math>\approx 10</math> s at 2000 g)</li> <li>• Incubation at room temperature for 1 h</li> </ul>	Stops alkylation by neutralizing remaining iodoacetamide
<ul style="list-style-type: none"> <li>• Addition of 5 <math>\mu\text{L}</math> of a 40 ng per <math>\mu\text{L}</math> trypsin solution</li> <li>• Incubation at 37 °C for 18 h</li> </ul>	Tryptic digestion of sample

Each digested solution was acidified by the addition of 1  $\mu\text{L}$  formic acid, and extracted with a modified tip (NuTip®, C18, 10  $\mu\text{L}$ ) according to the protocol<sup>96</sup> described in *Table 3.3*.



Table 3.3: Employed NuTip (NT1C18, 10  $\mu$ L) protocol to desalt and concentrate tryptic digests of collected fractions

Solvent/solution	Up&Down pipetting (number of repetitions)	Purpose
10 $\mu$ L acetonitrile	3	Pre-conditioning of NuTip®
10 $\mu$ L 0.1% formic acid	3	Solvent discarded after each repetition
Sample solution	10	Loading of ZipTip
10 $\mu$ L 0.1% formic acid	6	Washing step; Solvent discarded after each repetition
4 $\mu$ L 0.1% formic acid in 60% acetonitrile	10	Elution/concentration of retained sample

The concentrated and purified samples were spotted with CHCA in dried droplet (Table 2.2), and analyzed with the Ultraflex III ToF/ToF instrument. The system was used in the reflectron mode to obtain overview spectra of the tryptic digest fragments, and, additionally, molecules of abundant ion signals were fragmented in the LIFT mode to elucidate ion composition.<sup>58</sup>

### 3.1.8. Identification of putative biomarker through peptide sequence database search

As discussed in the introduction, a common approach to identify proteins is based on the analysis of peptide fragments of the target molecule(s) which are in a  $m/z$  range (<20 kDa) amenable to routine mass spectrometric analysis. The peptide fragments for this so-called “bottom-up” approach are obtained through proteolytic digestion of the sample.<sup>36</sup> The enzyme trypsin is widely employed for its stability under a wide range of conditions, and its high selectivity to cleave polypeptide chains at the C-terminal side of the amino acids arginine (R) and lysine (K).<sup>97</sup> This specificity of cleavage sites allows the prediction of fragments from protein sequences, so that matching the experimentally observed mass of the intact and the tryptic fragments can lead to the identification of the polypeptide. For this, however, the mass spectral data has to be searched against a peptide sequence data base that already contains protein sequence information of the investigated organism.<sup>37</sup> In this work, the search engine MASCOT<sup>98</sup> was used to match the mass spectral data against protein sequences from the UniProt

database.<sup>99</sup> To gain additional information on the analyte, and hence increase the confidence in the assignment, the PSD fragments of the tryptic peptides were investigated with the Ultraflex ToF/ToF in the LIFT mode, and this combined information was used in the data base search. The search criteria were set to “taxonomy: Rattus”, “enzyme: Trypsin”, “global modification: carbamidomethyl (C)” (fixed modification introduced in the digestion protocol), “variable modification: oxidation (M)”, “Mass tol. MS: 0.5 Da”, “Charge state: +1”, “monoisotopic”, and as instrument: “MALDI-TOF-TOF”.

### 3.1.9. Interpretation of PSD spectra – nomenclature and systematic

In the PSD of peptides, the majority of the formed fragment ions are the result of cleavage along the peptide’s backbone.<sup>100</sup> The mass spectral data on these can be used to elucidate information on the sequence of the intact parent peptide, as well as on potential modifications of the constituting amino acids.<sup>37</sup> *Figure 3.2* uses Biemann’s modified version<sup>101</sup> of the Roepstorff nomenclature,<sup>102</sup> displaying the generic polypeptide sequence of Alanine(A)-Glutamic acid(E)-Leucine(L)-Serine(S) to illustrate C- and N-terminal fragments produced by cleavage along the peptide bond. If the proton remains on the N-terminal fragment, b-type ions are produced, while remaining on the C-terminal fragment, y-type ions are observed. The index on each series further indicates how many amino acids the respective ion contains. Additional to this nomenclature, *Figure 3.2* also indicates the molecular composition of E and L along with the monoisotopic mass. It should be noted that, as opposed to the mass of individual amino acids, these masses are reduced by the mass of H<sub>2</sub>O. This so-called residual mass is due to formation of the peptide bonds within the polypeptide chain, and the concomitant elimination of one H-group at the N-terminus, and the OH-group at the C-terminus of the amino acids within the chain.

Consequently, the mass of an intact, protonated peptide is the sum of all the residual amino acid masses plus the mass of H<sub>2</sub>O (from both termini) and of one proton,  $[MH + H_2O]^+$  ( $M$  represents the sum of amino acid residues). Further, this explains that protonated ion fragments from the y-series would comprise  $[MH + OH]^+$ , while b-ions would be composed of  $[MH + H]^+$ , each representing the contribution of the related terminal group. The underlying polypeptide sequence can, ideally, be deduced by considering the mass difference of two ion fragments produced from cleavage of adjacent peptide bonds. So, in the depicted example, the mass difference of y<sub>3</sub> and y<sub>2</sub> fragment ions is the residual mass of E (129.04 Da), which is exactly what the comparison of b<sub>1</sub> and b<sub>2</sub> fragment ions would reveal. Thus, the sequence can be “read” from the mass spectrum through either fragment ion series, provided individual ion fragment intensity permits the assignment. Important here is that, in the interpretation, the difference is denoted as  $[M]$ ,  $[M + OH]$ , or  $[M + H]$ , without the proton and its charge.<sup>37</sup>

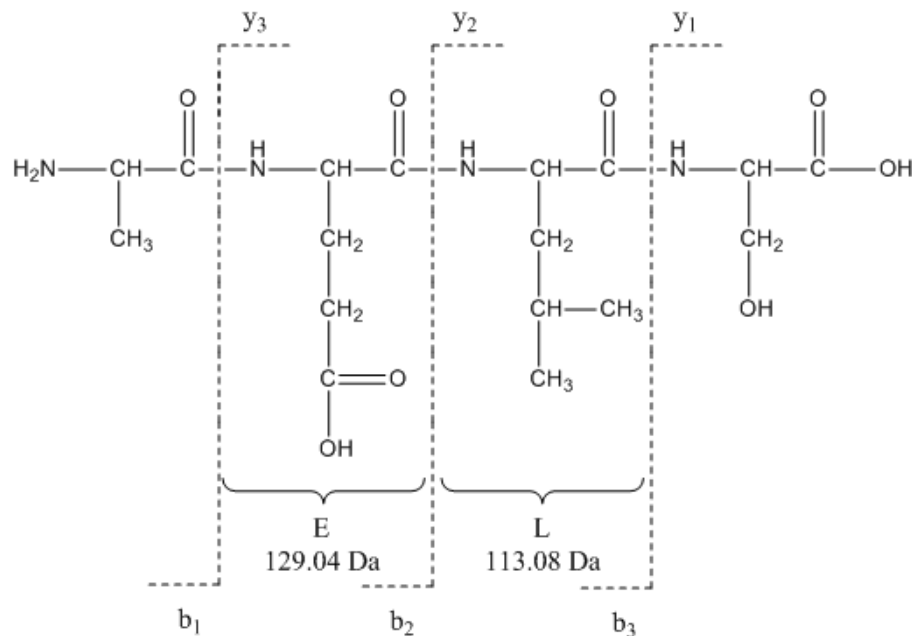


Figure 3.2: Polypeptide sequence of Alanine(A)-Glutamic acid(E)-Leucine(L)-Serine(S), illustrating b- and y-type ions produced by cleavage of peptide bonds. Brackets are used for E and L to indicate the composition comprising the residual mass of each amino acid along with the respective monoisotopic masses.

According to these rules, the PSD spectra produced from the LIFT mode were analyzed for y- and b-type ion series to confirm tryptic peptide fragment sequences obtained in the database search. Mass differences were annotated when observed difference were within  $\pm 0.05$  Da of the respective residual mass, and for ambiguous identifications, both residues were presented.

### 3.2. Results and discussion

*Figure 3.3* depicts an overview of base peak chromatograms (BPC) in the range of 0 to 25 minutes of lysates from quiescent (top), LPS activated (middle), and IL-4 activated (bottom) macrophages. Lysates were prepared as described above under 3.1.2. and separation was according to elution conditions in *Table 3.1*. As described above in 3.1.6. , the mass spectra constituting each chromatogram were individually investigated for the presence of reproducible ion signals ( $S/N < 5$ , and a minimum of 3 charge states per molecule).

In general, it should also be noted that the employed workflow is targeting hydrophilic molecules, which could be extracted from the sample with distilled water.

#### 3.2.1. Reproducibility of LC-MS signal intensity

*Table 3.4* summarizes the results of testing the LC-MS system for the reproducibility of ion signal intensity. For each eluting molecule, the average peak area of the respective EIC was calculated, and the corresponding relative standard deviation (RSD) is given. The tendency of increased RSD with lower relative peak area can be observed, indicating that more intense signals would serve as more robust indicator for the purpose of distinguishing activation states based on molecular fingerprints. The weighted RSD of 6.0% was calculated according to *Equation 3.1*, and illustrates the reproducibility of the employed LC-MS system with respect to ion signal intensity.

$$\text{Weighted RSD} = \sum_{i=0}^n \text{Relative peak area} \times \text{Relative standard deviation}$$

*Equation 3.1: Formula used to calculate the weighted RSD of n integrated peak areas*

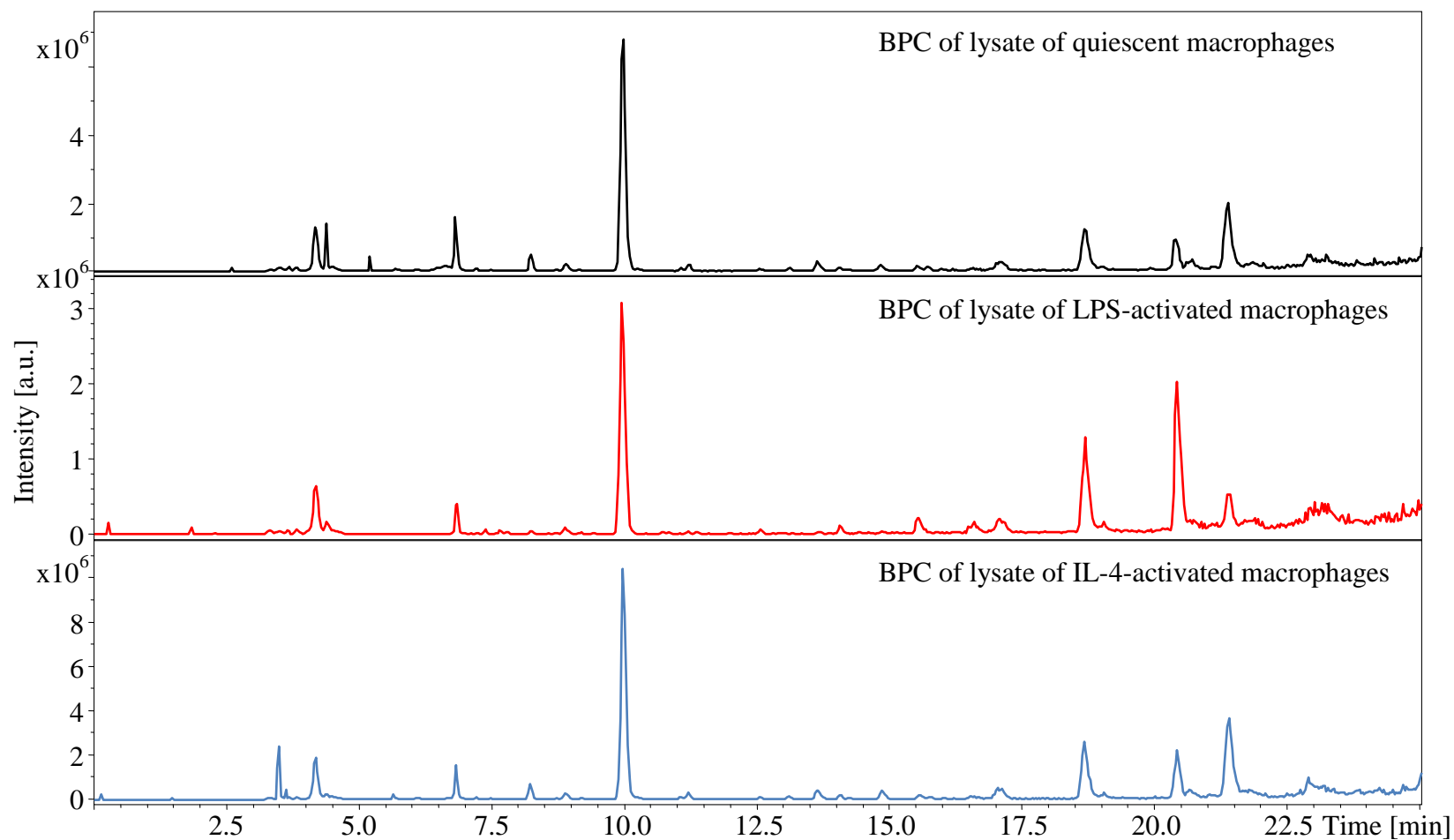


Figure 3.3: Representative base peak chromatograms (BPC) in the range of 0 to 25 minutes of lysates from quiescent (top), LPS activated (middle), and IL-4 activated (bottom) cells. Lysates were prepared according to 3.1.2. and separation was according to elution conditions in Table 3.1.

Table 3.4: Resulting relative standard deviations of ion signal obtained in LC-MS experiments on 30  $\mu$ L aliquots (three) of quiescent macrophage lysate.

Average retention time [min]	Area [a.u.]			Average area [a.u.]	Relative peak area	Relative standard deviation
8.6	7.50E+05	8.23E+05	8.29E+05	8.00E+05	0.48%	5.5%
10.0	8.26E+07	8.49E+07	8.86E+07	8.54E+07	50.79%	3.6%
11.3	1.16E+06	1.31E+06	1.75E+06	1.40E+06	0.83%	21.9%
13.1	7.55E+05	4.27E+05	6.47E+05	6.10E+05	0.36%	27.4%
13.7	2.64E+06	2.90E+06	2.91E+06	2.82E+06	1.68%	5.4%
14.9	1.98E+06	2.92E+06	3.12E+06	2.67E+06	1.59%	22.8%
16.6	6.45E+06	6.42E+06	5.58E+06	6.15E+06	3.66%	8.0%
18.8	2.91E+07	2.87E+07	3.16E+07	2.98E+07	17.73%	5.2%
20.4	2.50E+07	2.93E+07	2.63E+07	2.69E+07	15.99%	8.3%
21.3	1.06E+07	1.32E+07	1.10E+07	1.16E+07	6.90%	12.1%
<b>weighted relative standard deviation:</b>						<b>6.0%</b>

For each of the 10 eluting peaks, the EIC of all related charge states (ion signal in mass spectra S/N > 5, minimum of 3 charge states) in each technical replicate was integrated, and the relative standard deviation (RSD) of the average area was calculated. The relative peak area was calculated (average area of peak divided by sum of all average areas) and used to obtain the weighted RSD (sum of RSDs multiplied by relative peak areas) to account for the tendency of less intense signal to have a higher RSD. The weighted RSD illustrates the reproducibility of the ion signal intensities of the employed LC-MS system

### 3.2.2. Analysis of ion signals present under quiescent, IL-4 and LPS-induced condition

A statistical treatment of the data on IL-4 was not feasible, since only 4 biological replicates of this condition were analyzed, of which only two would have had a strong enough signal of the observed, eluting molecules, so only the quiescent and the LPS-induced condition were compared. *Table 3.5* gives an overview of all 9 common molecules detected by LC-MS of lysate from quiescent (white background) and LPS-induced (grey background) macrophages. The average relative areas and the related standard deviation for of each ion signal pair (quiescent and LPS-induced) were evaluated using t-tests (unpaired, two-tailed, equal variance or unequal variance (based on individual F-test). In each case, the difference was significant at the threshold level of  $p=0.01$ , suggesting that the obtained molecular fingerprint can be used to differentiate between lysates from quiescent and LPS-induced cell cultures.

### 3.2.3. Molecule eluting at minute 21.5 as strong indicator for LPS-induction of macrophages

Visually comparing the LC-MS chromatogram of quiescent and LPS-induced macrophages revealed one ion signal (eluting after  $\approx 21.5$ min) that was only present (at the threshold of  $S/N > 5$ ) in lysate from quiescent macrophages, but not from lysate obtained from LPS-induced ones. *Figure 3.4* displays a representative mass spectrum of this molecule, along with the mass spectra representing the other two prominent peaks (see *Figure 3.3.*) at minute 18.5 (top) and 20.0 (middle). The ion signals could be deconvoluted to obtain the ion masses of 8451.8 Da (top), 10815.9 Da (middle), and 3990.5 Da (bottom), which could be also confirmed through the fraction collection experiment, and the following MALDI experiment on the dried fractions (*Figure 3.6*, corresponding ions marked with a star).

Using the  $m/z$  of each charge state of each molecule highlighted in *Figure 3.4*, an extracted ion chromatogram (EIC) was generated for each LC-MS experiment on lysate from quiescent



and LPS-induced macrophages. *Figure 3.5* displays an overlay of EIC constructed this way of each 5 biological replicates lysate from quiescent (top) and LPS-induced macrophages (bottom), demonstrating the absence of the molecule eluting at minute 21.5 after activation with LPS.

Table 3.5: Summary of the relative peak areas of all 9 common molecules detected by LC-MS of lysate from quiescent (white background) and LPS-induced (grey background) macrophages.

<i>m/z</i> [Da]	Average RT [min]	Average, relative peak areas of signals found in lysate from quiescent (white background) and LPS-induced (grey background) macrophages [n = 10] [%]	Standard deviation	F-test	t-test
2664.7	7.5	1.80	0.51	8.75 x 10 <sup>-5</sup>	9.80 x 10 <sup>-6</sup> *
	7.5	0.44	0.11		
4964.0	9.9	46.94	6.76	8.65 x 10 <sup>-3</sup>	4.73 x 10 <sup>-4</sup> *
	9.9	35.94	2.59		
3790.9	11.2	1.06	0.20	4.55 x 10 <sup>-2</sup>	8.53 x 10 <sup>-10</sup>
	11.2	0.26	0.10		
4356.9	13.1	0.50	0.16	2.11 x 10 <sup>-3</sup>	2.82 x 10 <sup>-4</sup> *
	13.1	0.22	0.05		
4971.0	13.7	2.20	0.44	7.83 x 10 <sup>-2</sup>	1.08 x 10 <sup>-7</sup>
	13.7	0.87	0.23		
5199.4	14.9	2.24	0.57	1.08 x 10 <sup>-3</sup>	1.71 x 10 <sup>-6</sup> *
	14.9	0.47	0.16		
7886.7	16.6	2.20	0.55	7.88 x 10 <sup>-1</sup>	1.51 x 10 <sup>-3</sup>
	16.6	3.17	0.61		
8453.3	18.7	25.91	5.04	9.85 x 10 <sup>-1</sup>	2.07 x 10 <sup>-3</sup>
	18.7	34.04	5.07		
10816.9	20.4	17.15	1.88	1.25 x 10 <sup>-3</sup>	4.85 x 10 <sup>-3</sup> *
	20.4	24.59	6.36		

Experiments performed on 10 biological replicates each. The variance of each average relative peak area was compared (quiescent vs LPS-induced) with the F-test, and the means were accordingly evaluated using t-tests (unpaired, two-tailed, equal or unequal variance (based on the corresponding F-test, \* denotes unequal variance at p = 0.01)). For each molecule, the difference was significant at the threshold level of p=0.01.

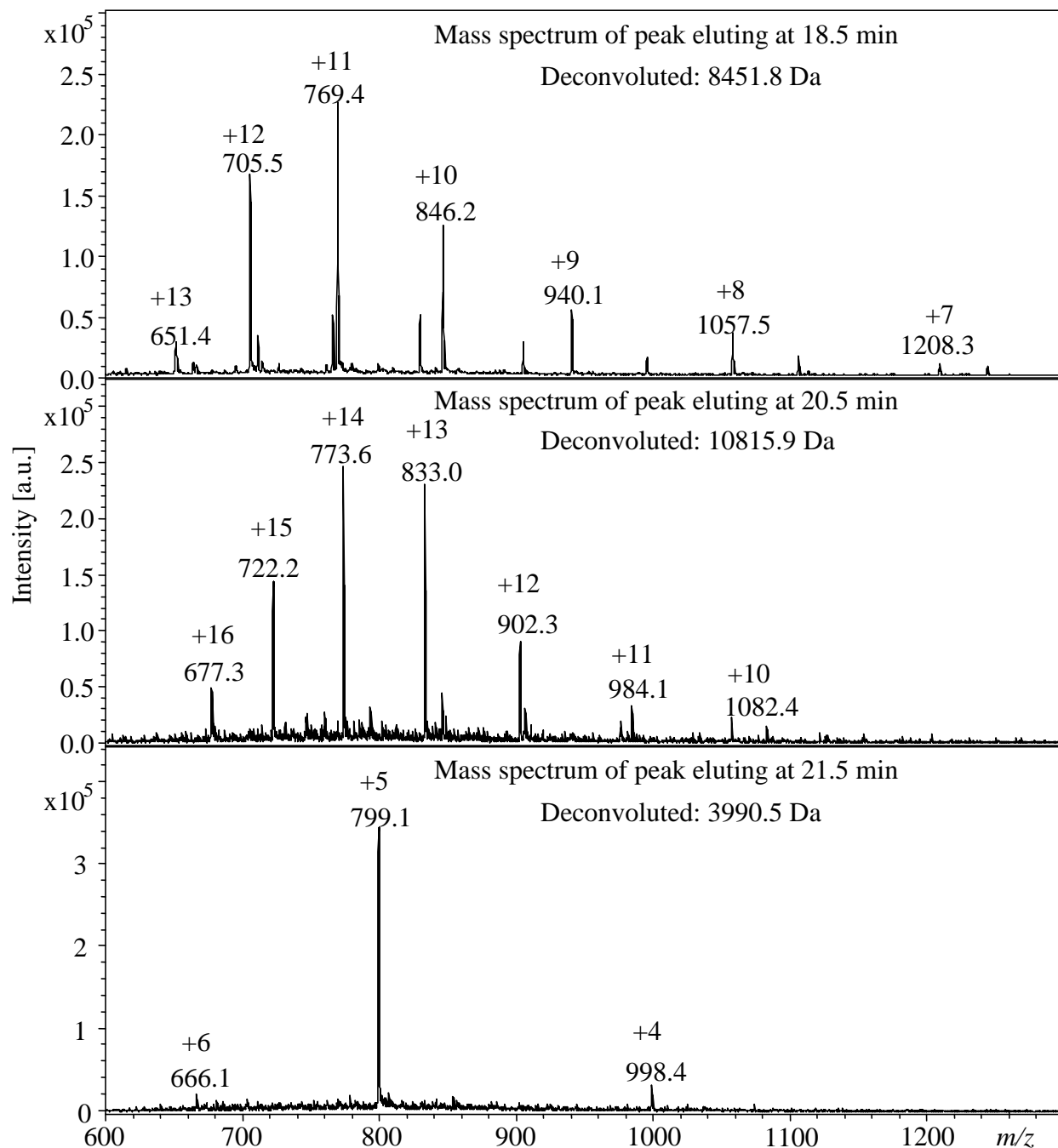


Figure 3.4: Representative mass spectra from a LC-MS experiment on quiescent macrophage lysate. The spectra are of the three prominent peaks (see Figure 3.3.) at minute 18.5 min (top), 20.0 min (middle), and 21.5 min (bottom). The ion peaks are additionally labeled with the calculated charge states, and the deconvoluted masses are given as 8451.8 Da (top), 10815.9 Da (middle), and 3990.5 Da (bottom).

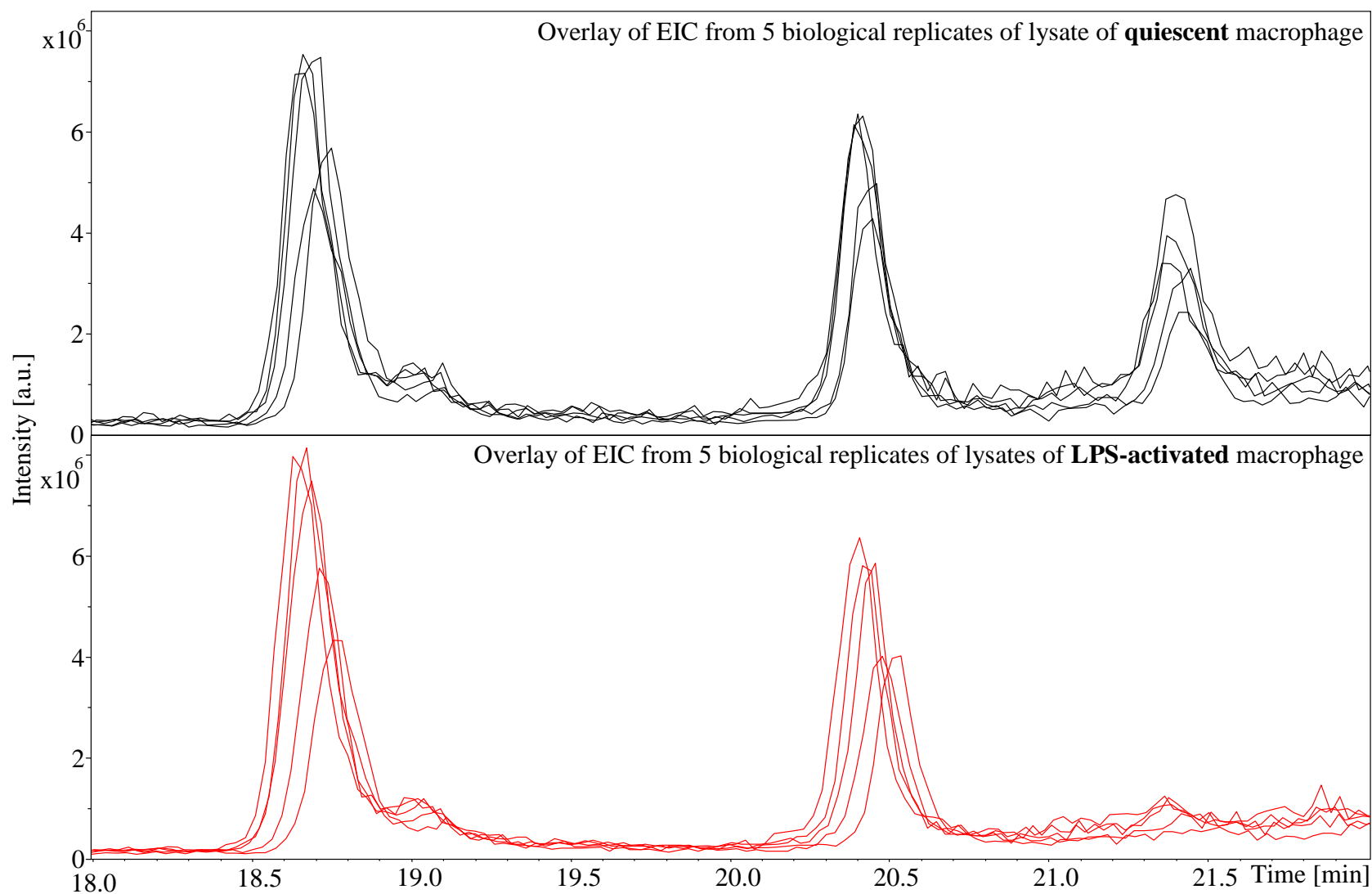


Figure 3.5: Overlay of extracted ion chromatograms (EIC) obtained from lysate of quiescent (top) and LPS-activated macrophages (5 biological replicates each), demonstrating the absence of the molecule eluting at minute  $\approx 21.5$ . The lysates were separated according to Table 3.1, and the EIC were constructed by integrating all displayed  $m/z$  ( $\pm 0.5$  Da) in Figure 3.4.

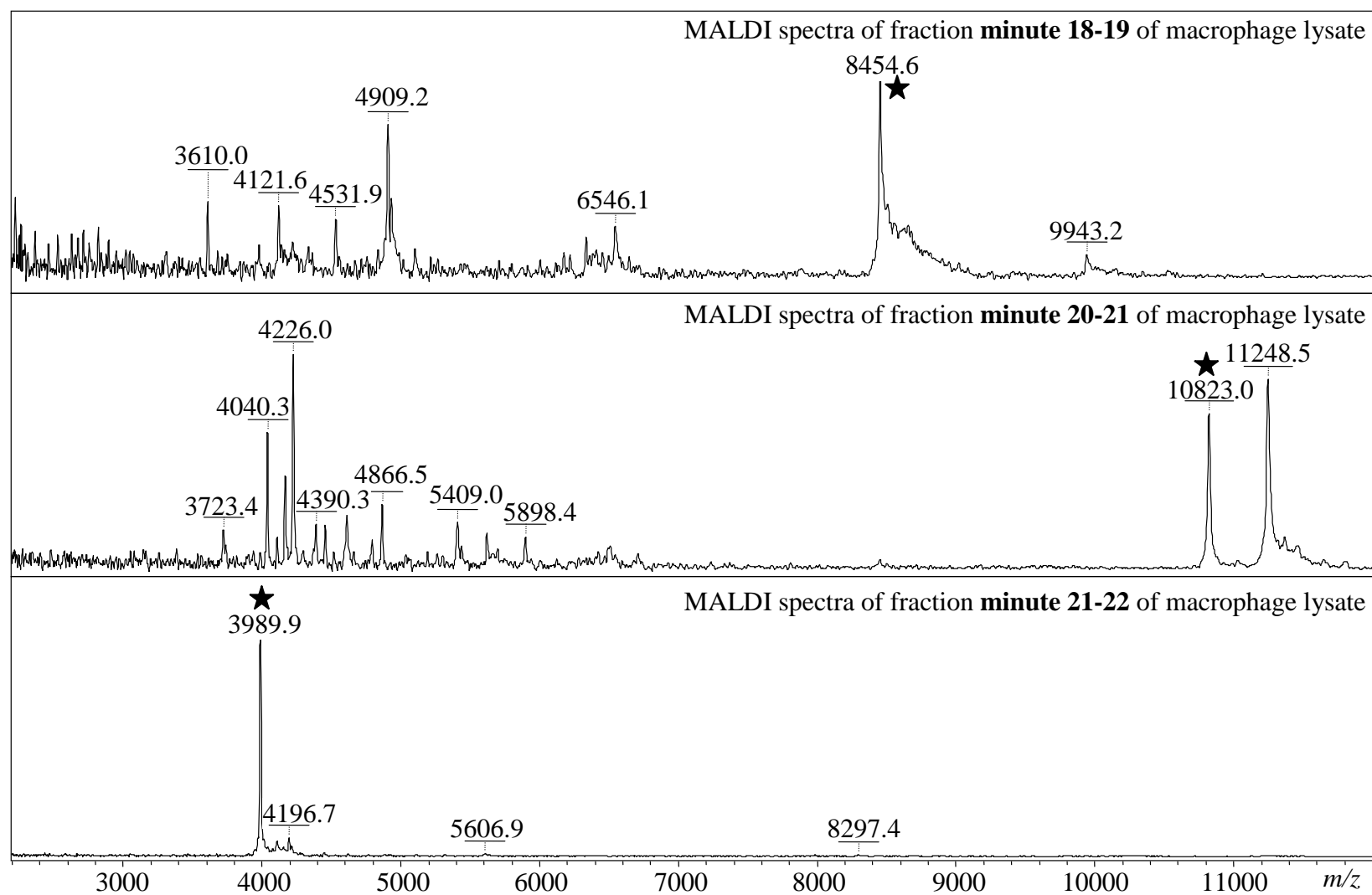


Figure 3.6: MALDI mass spectra of macrophage lysate fractions collected at minute 18-19 (top), minute 20-21 (middle), and minute 21-22 (bottom). Ion signals corresponding to the dominant ESI-MS signal (Figure 3.4) are highlighted with a star in the respective spectrum. Lysate fraction were prepared in SA, as described above (3.1.5. )

#### 3.2.4. Identification of putative biomarker for LPS-activation as macrophage-capping protein

*Figure 3.7* gives an overview of the information obtained on the intact molecule eluting at minute  $\approx 21.5$ . Since the absence of this molecule indicates LPS-activation, the presented data is on lysate from quiescent macrophages where the molecule is detectable. The bottom right displays an ESI mass spectrum, while the bottom left depicts the MALDI mass spectrum of the corresponding dried fraction. The ESI signal deconvolutes to the average molecule mass of 3990.5 Da, while the MALDI data shows the monoisotopic mass of 3988.4 Da. This slight difference in mass is based on the mathematical nature of averaging the  $m/z$  signal in the case of the ESI signal (i.e. unresolved isotopic pattern) vs the isotopically resolved MALDI spectrum (ToF instrument was used in reflectron mode). Further, the MALDI spectrum exhibits another peak lower in mass with the difference in mass matching the atomic mass of one oxygen atom (=16.0 Da), suggesting that the base peak contains one oxidized group.

*Figure 3.8* depicts the mass spectrum obtained on the tryptic digest of the biomarker containing fraction. The inset further presents the sequence of the protein fragment (amino acid position 305-339, which represents 7% of the entire protein sequence) of the protein “macrophage-capping protein”, which was the only significant ( $p < 0.05$ ) result of the data base search. The theoretical, protonated, and oxidized mass of this sequence, 3988.1 Da, is in very good agreement with the experimentally observed mass of 3988.4 Da (*Figure 3.7*). The two predicted tryptic fragments of 1375.7 Da and 1601.8 Da, which cover 77% of the depicted sequence, are both present in the spectrum (1375.7 Da and 1601.7 Da, respectively). To confirm this assignment, the PSD spectra of both tryptic fragments were analyzed based on the suggested sequence.

*Figure 3.9* depicts the PSD spectrum of the ion isolated at 1375.7 Da (isolation window +/- 3%). The sequence elucidated from the annotated b-ion series supports the assignment, and is further backed by the prominent peak at 579.1 Da representing the  $y_5$  fragment ion. Additionally, the theoretical ion mass differences are in excellent agreement (within 0.2 Da error) of the observed mass differences. It has to be noted that the amino acids lysine (K) and glutamine (Q), with a residual mass difference of 0.03 Da, cannot be unambiguously assigned, nor the stereo isomers leucine (L) and isoleucine (I).

*Figure 3.8* depicts the PSD spectrum of the ion isolated at 1601.7 Da (+/- 3%). The sequence elucidated from the annotated y-ion series supports the suggested sequence, and the theoretical ion mass differences compare very well (within 0.7 Da error) with experimentally observed differences.

In conclusion, the identification of the putative biomarker as part of the macrophage-capping protein can be supported on multiple levels. Through the excellent agreement of the theoretical and observed intact and tryptic fragments masses. Further, through the presence of these tryptic fragments with specificity of each fragment as being the product of the cleavage of each C-terminal arginine (R), and the total sequence coverage of 77% through both tryptic fragments. The postulated sequence is further validated through the presence of the annotated sequence-specific fragments in the PSD experiments.

The sequence of the complete protein was originally obtained from a large-scale cDNA project,<sup>103</sup> and the human ortholog was described by Dabiri et al. to be abundantly expressed only by macrophages.<sup>104</sup> Further, the observed behavior of this molecule being absent within the macrophages upon activation with LPS is demonstrated through complimentary results from Eichelbaum et al.<sup>31</sup> In their study targeting the protein synthesis and secretion during

macrophage activation of RAW 264.7 (mouse macrophage), they could show that the mouse ortholog of the macrophage capping protein was not newly synthesized upon stimulation with LPS (within 8 h after stimulation), but that it was released from the macrophages into the culture medium (8 h after stimulation, LPS stimulated media contained approximately 5.5 times more of the compound identified as macrophage capping protein than the quiescent control macrophages).<sup>31</sup> If similar behavior of the investigated rat macrophages can be assumed, this confirms the observation of this study that upon LPS stimulation, the peptide related to the macrophage capping protein is not found (below level of detection) within the macrophage lysate.



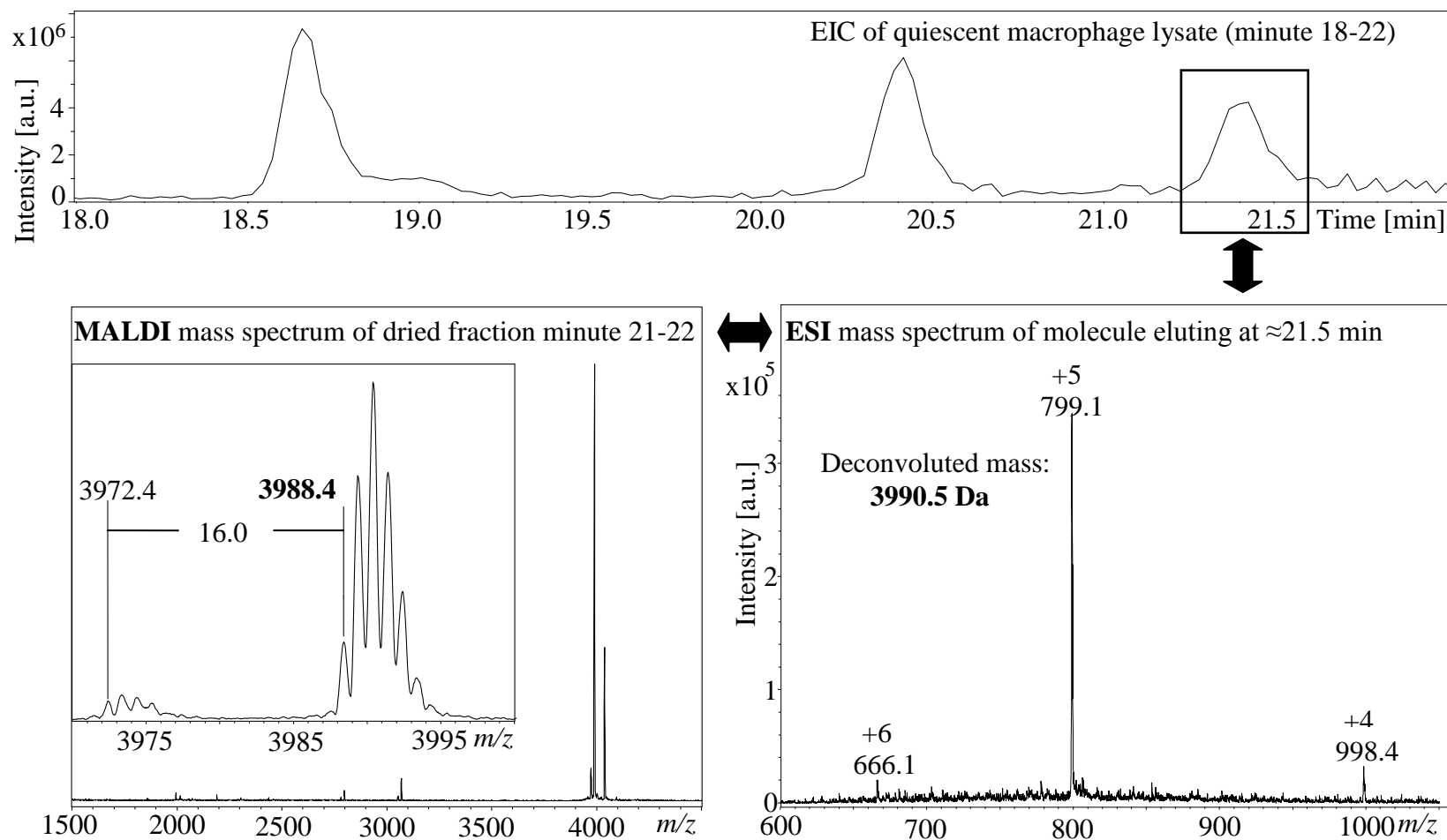
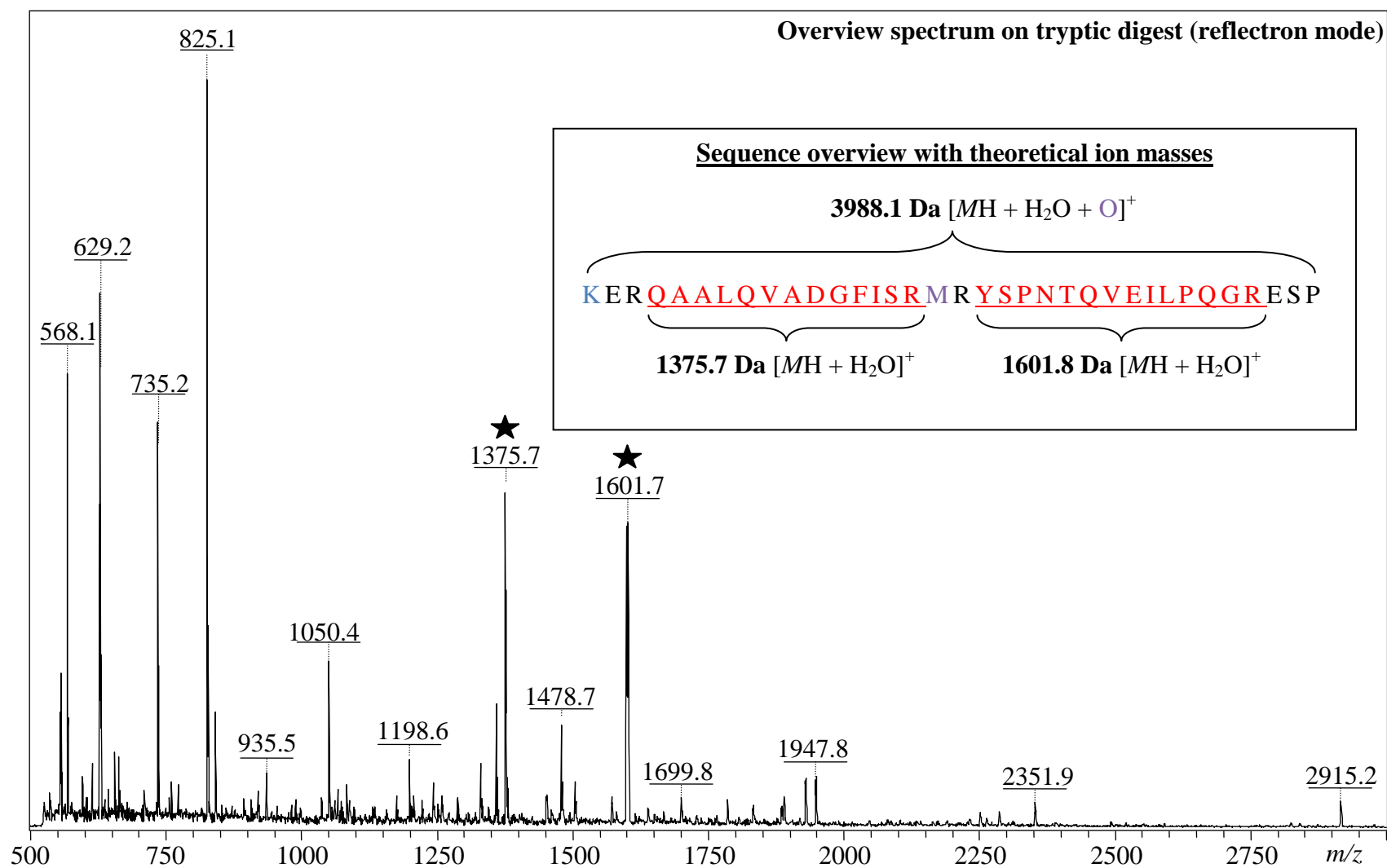


Figure 3.7: Overview of representative mass spectra collected on the putative biomarker. The top displays an EIC of lysate from quiescent macrophages with the signal corresponding to the molecule eluting at minute  $\approx 21.5$  highlighted. The bottom right displays the ESI mass spectrum with the deconvoluted  $m/z$  of 3990.5 Da, while the bottom left depicts an isotopically resolved (ToF in reflectron mode) MALDI mass spectrum of the corresponding dried fraction spotted in SA. The inset of the MALDI spectrum shows the enlarged range from 3974-3996  $m/z$ , exhibiting the monoisotopic peak (3988.4 Da) of the base peak, and an adjacent peak at 3972.39 Da. The difference of 16.0 Da suggests the presence of an additional oxygen atom (=16.0 Da). Note: the mass spectra are of lysate from **quiescent** macrophages, but the absence of this signal serves as indication for LPS-activation.



*Figure 3.8: Mass spectrum of tryptic fragments from the digestion experiment on the fraction containing the putative biomarker. The inset contains the sequence fragment (amino acid position 305-339) returned in the MASCOT database search of the depicted spectrum. The theoretical masses of the entire sequence, as well as of both tryptic fragments are indicated.*

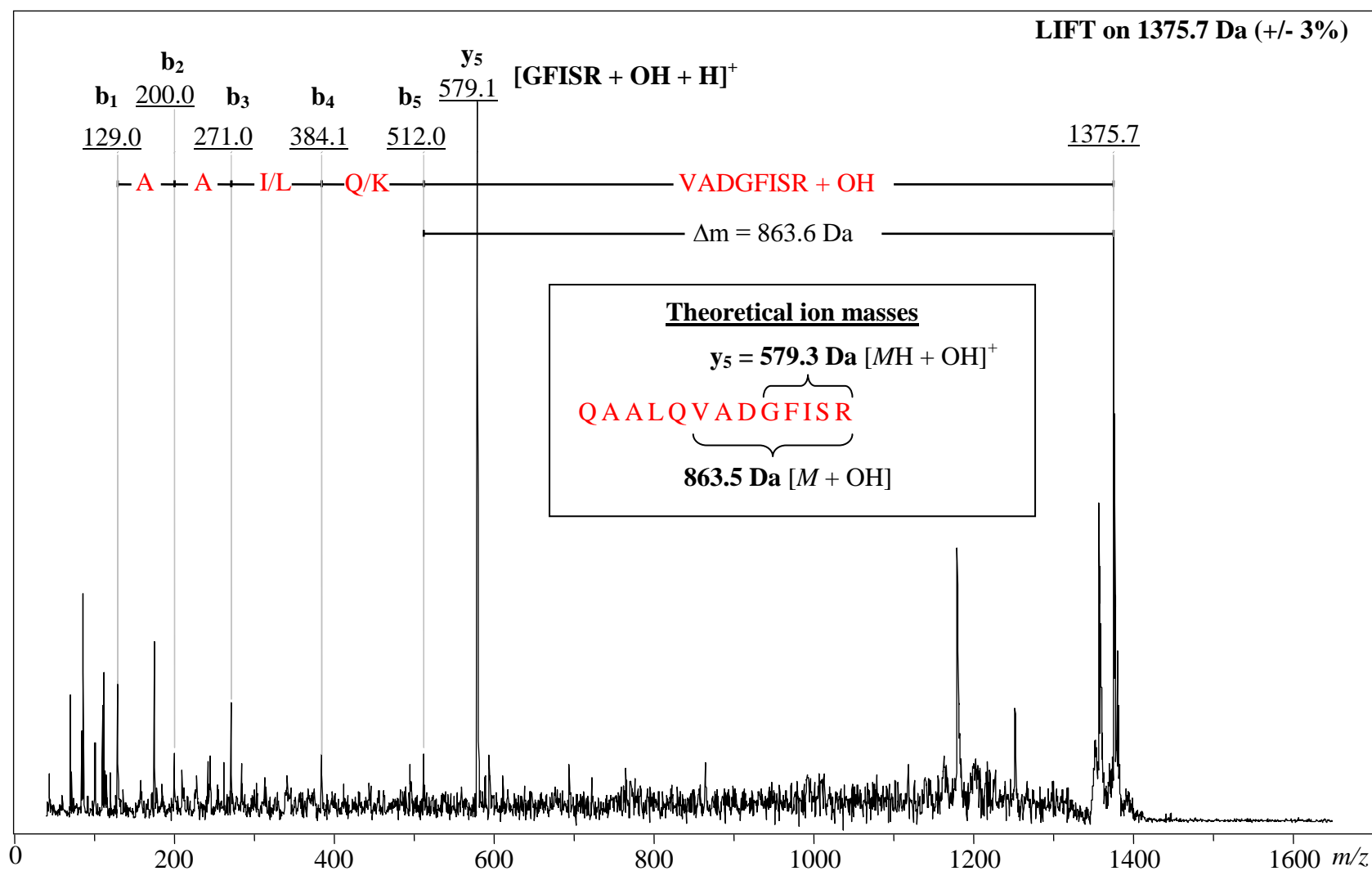


Figure 3.9: LIFT spectrum of ion 1375.7 Da (isolation window of +/- 3%) exhibiting mainly b-ion series fragments. The spectrum is annotated with amino acids corresponding to observed mass differences along with the theoretical values of the respective sequences in the inset. Additionally, the dominant peak at 579.1 Da is labeled as the  $y_5$  ion. Ambiguity in assignment is indicated by providing both potential amino acids. The obtained sequence information supports the proposed sequence for this tryptic fragment.

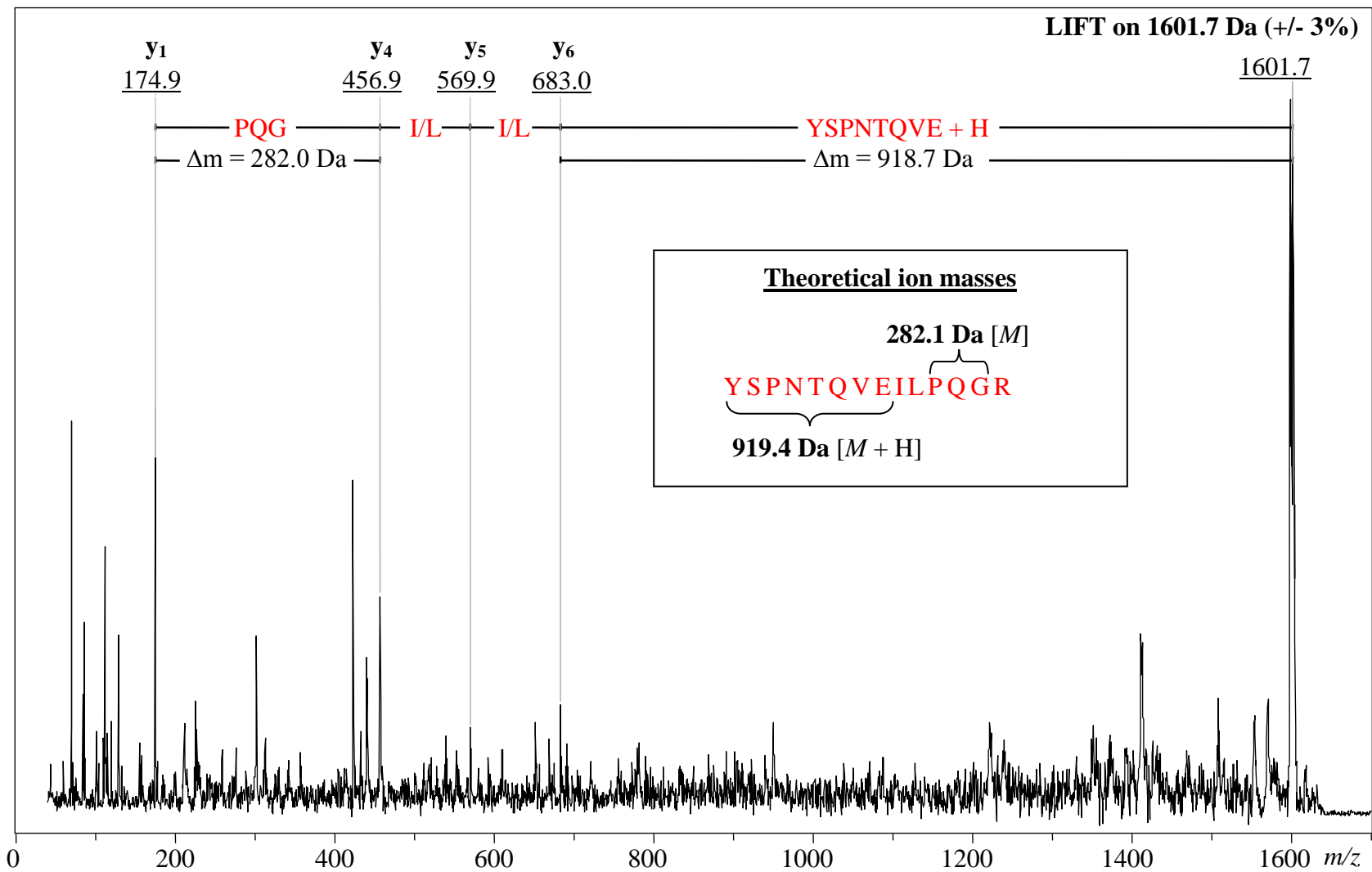


Figure 3.10: LIFT spectrum of ion 1601.7 Da (isolation window of +/- 3%) exhibiting y-ion series fragments. The spectrum is annotated with amino acids corresponding to observed mass differences along with the theoretical values of the respective sequences in the inset. The obtained sequence information supports the proposed sequence for this tryptic fragment.

## Chapter 4: Summary and future direction

Macrophages are versatile and highly adaptive cells that are involved in a wide range of physiological processes ranging from host defense, over homeostasis or regeneration, to pathogenesis.<sup>3-5,12,31,32,44,45,47</sup> They react to their microenvironment, assuming various roles based on chemical and/or physical cues.<sup>1,3,6,7,16</sup> It has been proposed that macrophages exist along a continuous spectrum in between these so-called activation states,<sup>13</sup> and it was shown that macrophages can be reversibly shifted between activation states.<sup>15-17,19</sup> Since the microenvironment is significant to macrophage activation, it is desirable to obtain information on spatial distribution along with the activation state of macrophages on tissue sections. This information is currently predominantly obtained through an immunohistochemistry approach.<sup>50</sup>

The aim of this work was to explore the application of mass spectrometry to the task of distinguishing macrophage activation states. The assumption that significant differences in molecular composition correlates with observed activation states is based on high-throughput proteomics experiments, revealing distinct protein levels attributed to activation with LPS.<sup>30,31</sup> The intention was to investigate whether MALDI MS conditions could be found that permit identification of macrophage activation states within tissue sections.

In Chapter 2, the sample preparation technique of matrix-assisted laser desorption/ionization (MALDI) was explored to evaluate its use for MALDI imaging mass spectrometry (IMS) experiments, which could reveal activation state, spatial distribution, and concentration of macrophages within tissue sections. As model, the immortalized macrophage cell line NR8383 (rat, alveolar) was cultured and *in vitro* activated with either the cytokine IL-4, or the endotoxin LPS. Despite varying core parameters like the employed matrices, sample preparation techniques, and employed solvents for sample extraction, no reproducible mass spectral

fingerprint of macrophage was observed that could indicate a difference in the induced activation state. It could be observed that the mass spectral fingerprint, especially in the range of 4000 – 6500  $m/z$  (compare inset *Figure 2.3*), appeared to be well conserved across differing activation states (*Figure 2.9*), differing extraction solvents (*Figure 2.6*), and, to a certain degree, across different employed matrices (*Figure 2.1*). It was concluded that, despite the reported differences in molecular composition correlating LPS activation, the signals from these biomarkers were suppressed by the relative strong ionizability of the molecules constituting this conserved mass spectral fingerprint.

Chapter 3 describes the introduction of high-performance liquid chromatography (HPLC) as a mean to reduce the molecular sample complexity, as well as electrospray ionization (ESI) as an alternative to MALDI as the mass spectrometry source. Comparison of normalized signal intensities obtained on macrophage lysate from quiescent and LPS-induced in the LC-ESI-MS experiments revealed reproducible differences in the relative intensities of the eluting compounds. Within 10 biological replicates of the LPS-activated vs the quiescent state separated under identical elution conditions, the relative ion intensities of 9 common ions were compared. A significant ( $p < 0.01$ ) difference was observed for each common ion, suggesting that the 30 min separation protocol would allow distinguishing quiescent from LPS-activated macrophages based on the relative abundance of the investigated signal (*Table 3.5*). However, a molecule eluting after 21.5 min could be recognized as strong indicator for LPS activation. In lysate from quiescent macrophages, the corresponding signal contributed 9 % ( $\pm$  1% standard deviation) of relative ion signal, while the signal upon LPS activation was absent (*Figure 3.5*). The average molecular mass of this putative biomarker was measured by ESI MS to be 3990.5 Da, and confirmed by the monoisotopic mass of 3988.4 Da measured in a MALDI experiment of the

corresponding, collected, and dried fraction (*Figure 3.7*). MALDI experiments on the tryptic digest containing the putative biomarker supports the identification of it as peptide corresponding to the amino acid sequence (position 305-339) of the macrophage-capping protein. This finding is conclusive with the observations made in a proteomics experiment on LPS-induced macrophages (RAW 264.7, mouse).

Based on the identification of this peptide, further work could include its use as an alternative indicator for LPS-activation of macrophages. For this, the presence of this marker in macrophages harvested from various tissues and organisms would have to be established, as well as its absence under LPS-activation. Based on the observation that the peptide is soluble in water (as used for the extraction), but will adhere to the column material ( $\emptyset$  5  $\mu\text{m}$  particles, modified with  $\text{C}_{18}$ , and containing 300  $\text{\AA}$  micro pores), and will only elute after reaching approximately 36% acetonitrile content, could be used to concentrate and detect it from media with the help of accordingly modified pipette tips.<sup>105</sup>

Further, based on the high specificity of this biomarker for macrophages,<sup>104</sup> it could be used for mapping of the spatial distribution of quiescent macrophages on tissue sections. For this, liquid extraction based mass spectrometry methods have been proposed as alternative for the analysis of tissue sections,<sup>85-87</sup> as well as automated, semi-continuous techniques compatible with HPLC<sup>88-90</sup> could be used.

## References

1. Burke B, Lewis CE, eds. *The macrophage*. 2nd ed. Oxford University Press; 2002.
2. Roslin Institute. Macrophages.com - the macrophage community website. <http://www.macrophages.com/home>. Updated 2014. Accessed 09/18, 2014.
3. Murray PJ, Wynn TA. Protective and pathogenic functions of macrophage subsets. *Nat Rev Immunol*. 2011;11(11):723-737.
4. Janeway C, Travers P, Walport M, Shlomchik M. *Immunobiology - the immune system in health and disease*. Sixth ed. New York: Garland Science; 2004.
5. Brancato SK, Albina JE. Wound macrophages as key regulators of repair: Origin, phenotype, and function. *Am J Pathol*. 2011;178(1):19-25.
6. Gordon S, Martinez FO. Alternative activation of macrophages: Mechanism and functions. *Immunity*. 2010;32(5):593-604.
7. Murray PJ, Allen JE, Biswas SK, et al. Macrophage activation and polarization: Nomenclature and experimental guidelines. *Immunity*. 2014;41(1):14-20.
8. Fildes P. Richard friedrich johannes pfeiffer. 1858-1945. *Biogr Mem Fellows R Soc*. 1956;2:237-247.
9. Mantovani A, Sica A, Locati M. Macrophage polarization comes of age. *Immunity*. 2005;23(4):344-346.
10. Stein M, Keshav S, Harris N, Gordon S. Interleukin 4 potently enhances murine macrophage mannose receptor activity: A marker of alternative immunologic macrophage activation. *J Exp Med*. 1992;176(1):287-292.
11. Edwards JP, Zhang X, Frauwirth KA, Mosser DM. Biochemical and functional characterization of three activated macrophage populations. *J Leukocyte Biol*. 2006;80(6):1298-1307.
12. Loke P, Gallagher I, Nair MG, et al. Alternative activation is an innate response to injury that requires CD4+ T cells to be sustained during chronic infection. *J Immunol*. 2007;179(6):3926-3936.
13. Mosser DM, Edwards JP. Exploring the full spectrum of macrophage activation. *Nat Rev Immunol*. 2008;8(12):958-969.
14. Mills CD, Kincaid K, Alt JM, Heilman MJ, Hill AM. M-1/M-2 macrophages and the Th1/Th2 paradigm. *J Immunol*. 2000;164(12):6166-6173.



15. Rutschman R, Lang R, Hesse M, Ihle JN, Wynn TA, Murray PJ. Cutting edge: Stat6-dependent substrate depletion regulates nitric oxide production. *J Immunol.* 2001;166(4):2173-2177.
16. Stout RD, Suttles J. Functional plasticity of macrophages: Reversible adaptation to changing microenvironments. *J Leukocyte Biol.* 2004;76(3):509-513.
17. Stout RD, Jiang C, Matta B, Tietzel I, Watkins SK, Suttles J. Macrophages sequentially change their functional phenotype in response to changes in microenvironmental influences. *J Immunol.* 2005;175(1):342-349.
18. Hagemann T, Lawrence T, McNeish I, et al. "Re-educating" tumor-associated macrophages by targeting NF- $\kappa$ B. *J Exp Med.* 2008;205(6):1261-1268.
19. Kawanishi N, Yano H, Yokogawa Y, Suzuki K. Exercise training inhibits inflammation in adipose tissue via both suppression of macrophage infiltration and acceleration of phenotypic switching from M1 to M2 macrophages in high-fat-diet-induced obese mice. *Exerc Immunol Rev.* 2010;16:105-118.
20. Nelson DL, Cox MM, eds. *Lehninger principles of biochemistry.* 4th ed. New York: W. H. Freeman and Company; 2005.
21. Ramsey SA, Klemm SL, Zak DE, et al. Uncovering a macrophage transcriptional program by integrating evidence from motif scanning and expression dynamics. *PLoS Comput Biol.* 2008;4(3):e1000021.
22. Litvak V, Ramsey SA, Rust AG, et al. Function of C/EBP $\delta$  in a regulatory circuit that discriminates between transient and persistent TLR4-induced signals. *Nat Immunol.* 2009;10(4):437-443.
23. Zhu X, Chang MS, Hsueh RC, et al. Dual ligand stimulation of RAW 264.7 cells uncovers feedback mechanisms that regulate TLR-mediated gene expression. *J Immunol.* 2006;177(7):4299-4310.
24. Bhatt DM, Pandya-Jones A, Tong A, et al. Transcript dynamics of proinflammatory genes revealed by sequence analysis of subcellular RNA fractions. *Cell.* 2012;150(2):279-290.
25. Weintz G, Olsen JV, Frühauf K, et al. The phosphoproteome of toll-like receptor-activated macrophages. *Mol Syst Biol.* 2010;6(1):1-16.
26. Sharma K, Kumar C, Kéri G, Breikopf SB, Oppermann FS, Daub H. Quantitative analysis of kinase-proximal signaling in lipopolysaccharide-induced innate immune response. *J Proteome Res.* 2010;9(5):2539-2549.
27. Patel PC, Fisher KH, Yang EC, Deane CM, Harrison RE. Proteomic analysis of microtubule-associated proteins during macrophage activation. *Mol Cell Proteomics.* 2009;8(11):2500-2514.

28. Dhungana S, Merrick BA, Tomer KB, Fessler MB. Quantitative proteomics analysis of macrophage rafts reveals compartmentalized activation of the proteasome and of proteasome-mediated ERK activation in response to lipopolysaccharide. *Mol Cell Proteomics*. 2009;8(1):201-213.
29. Brown J, Wallet MA, Krastins B, Sarracino D, Goodenow MM. Proteome bioprofiles distinguish between M1 priming and activation states in human macrophages. *J Leukocyte Biol*. 2010;87(4):655-662.
30. Meissner F, Scheltema RA, Mollenkopf HJ, Mann M. Direct proteomic quantification of the secretome of activated immune cells. *Science*. 2013;340(6131):475-478.
31. Eichelbaum K, Krijgsveld J. Rapid temporal dynamics of transcription, protein synthesis, and secretion during macrophage activation. *Mol Cell Proteomics*. 2014;13(3):792-810.
32. Joyce AR, Palsson BØ. The model organism as a system: Integrating 'omics' data sets. *Nat Rev Mol Cell Biol*. 2006;7(3):198-210.
33. Schena M, Shalon D, Davis RW, Brown PO. Quantitative monitoring of gene expression patterns with a complementary DNA microarray. *Science*. 1995;270(5235):467-470.
34. Gibson G, Muse SV, eds. *A primer of genome science*. 1st ed. Sunderland, Massachusetts: Sinauer Associates, Inc; 2002.
35. Takahashi N, Isobe T. *Proteomic biology using LC-MS : Large scale analysis of cellular dynamics and function*. Hoboken, New Jersey: Wiley-Interscience; 2008.
36. Wisniewski JR, Zougman A, Nagaraj N, Mann M. Universal sample preparation method for proteome analysis. *Nature methods*. 2009;6(5):359-363.
37. Watson JT, Sparkman OD, eds. *Introduction to mass spectrometry : Instrumentation, applications and strategies for data interpretation*. 4th ed. ed. Great Britain: John Wiley & Sons Ltd; 2007.
38. Pan Q, Shai O, Lee LJ, Frey BJ, Blencowe BJ. Deep surveying of alternative splicing complexity in the human transcriptome by high-throughput sequencing. *Nat Genet*. 2008;40(12):1413-1415.
39. Stastna M, Van Eyk JE. Analysis of protein isoforms: Can we do it better? *Proteomics*. 2012;12(19-20):2937-2948.
40. Vendrame E, Hussain SK, Breen EC, et al. Serum levels of cytokines and biomarkers for inflammation and immune activation, and HIV-associated non-hodgkin B-cell lymphoma risk. *Cancer Epidemiol Biomarkers Prev*. 2014;23(2):343-349.

41. Engvall E, Perlmann P. Enzyme-linked immunosorbent assay (ELISA) quantitative assay of immunoglobulin G. *Immunochemistry*. 1971;8(9):871-874.
42. Pollard JW. Trophic macrophages in development and disease. *Nat Rev Immunol*. 2009;9(4):259-270.
43. Wynn TA, Chawla A, Pollard JW. Macrophage biology in development, homeostasis and disease. *Nature*. 2013;496(7446):445-455.
44. Sindrilaru A, Peters T, Wieschalka S, et al. An unrestrained proinflammatory M1 macrophage population induced by iron impairs wound healing in humans and mice. *J Clin Invest*. 2011;121(3):985-997.
45. Wynn TA. Fibrotic disease and the TH1/TH2 paradigm. *Nat Rev Immunol*. 2004;4(8):583-594.
46. Wynn TA, Barron L. Macrophages: Master regulators of inflammation and fibrosis. *Semin Liver Dis*. 2010;30(3):245-257.
47. Chawla A, Nguyen KD, Goh YS. Macrophage-mediated inflammation in metabolic disease. *Nat Rev Immunol*. 2011;11(11):738-749.
48. Sica A, Bronte V. Altered macrophage differentiation and immune dysfunction in tumor development. *J Clin Invest*. 2007;117(5):1155-1166.
49. Duluc D, Corvaisier M, Blanchard S, et al. Interferon- $\gamma$  reverses the immunosuppressive and protumoral properties and prevents the generation of human tumor-associated macrophages. *Int J Cancer*. 2009;125(2):367-373.
50. Brown BN, Londono R, Tottey S, et al. Macrophage phenotype as a predictor of constructive remodeling following the implantation of biologically derived surgical mesh materials. *Acta Biomater*. 2012;8(3):978-987.
51. Brown BN, Ratner BD, Goodman SB, Amar S, Badylak SF. Macrophage polarization: An opportunity for improved outcomes in biomaterials and regenerative medicine. *Biomaterials*. 2012;33(15):3792-3802.
52. Nuovo GJ. *In situ molecular pathology and co-expression analyses*. Academic Press; 2013.
53. Brown BN, Valentin JE, Stewart-Akers AM, McCabe GP, Badylak SF. Macrophage phenotype and remodeling outcomes in response to biologic scaffolds with and without a cellular component. *Biomaterials*. 2009;30(8):1482-1491.
54. Karas M, Bachmann D, Hillenkamp F. Influence of the wavelength in high-irradiance ultraviolet laser desorption mass spectrometry of organic molecules. *Anal Chem*. 1985;57(14):2935-2939.

55. Hillenkamp F, Jaskolla TW, Karas M. The MALDI process and method. In: Hillenkamp F, Peter-Katalinic J, eds. *MALDI MS: A practical guide to instrumentation, methods, and applications*. Wiley-VCH Verlag GmbH & Co. KGaA; 2013:1-40. 10.1002/9783527335961.ch1.
56. Knochenmuss R, Zhigilei LV. What determines MALDI ion yields? A molecular dynamics study of ion loss mechanisms. *Anal Bioanal Chem*. 2012;402(8):2511-2519.
57. Kaufmann R, Kirsch D, Spengler B. Sequencing of peptides in a time-of-flight mass spectrometer: Evaluation of postsource decay following matrix-assisted laser desorption ionisation (MALDI). *Int J Mass Spectrom Ion Processes*. 1994;131:355-385.
58. Suckau D, Resemann A, Schuerenberg M, Hufnagel P, Franzen J, Holle A. A novel MALDI LIFT-TOF/TOF mass spectrometer for proteomics. *Anal Bioanal Chem*. 2003;376(7):952-965.
59. Heeren R, Smith DF, Stauber J, Kükrer-Kaletas B, MacAleese L. Imaging mass spectrometry: Hype or hope? *J Am Soc Mass Spectrom*. 2009;20(6):1006-1014.
60. Cornett DS, Reyzer ML, Chaurand P, Caprioli RM. MALDI imaging mass spectrometry: Molecular snapshots of biochemical systems. *Nat Methods*. 2007;4(10):828-833.
61. Hardesty WM, Caprioli RM. In situ molecular imaging of proteins in tissues using mass spectrometry. *Anal Bioanal Chem*. 2008;391(3):899-903.
62. Goodwin RJA. Sample preparation for mass spectrometry imaging: Small mistakes can lead to big consequences. *J Proteomics*. 2012;75(16):4893-4911.
63. Ifa DR, Wu C, Ouyang Z, Cooks RG. Desorption electrospray ionization and other ambient ionization methods: Current progress and preview. *Analyst*. 2010;135(4):669-681.
64. Wilkins CL, Lay JO, Jr. *Identification of microorganisms by mass spectrometry*. Vol 169. New York: John Wiley & Sons, Inc.; 2006.
65. Munteanu B, Hopf C. Emergence of whole-cell MALDI-MS biotyping for high-throughput bioanalysis of mammalian cells? *Bioanalysis*. 2013;5(8):885-893.
66. Karger A, Bettin B, Lenk M, Mettenleiter TC. Rapid characterisation of cell cultures by matrix-assisted laser desorption/ionisation mass spectrometric typing. *J Virol Methods*. 2010;164(1-2):116-121.
67. Ouedraogo R, Daumas A, Ghigo E, Capo C, Mege J, Textoris J. Whole-cell MALDI-TOF MS: A new tool to assess the multifaceted activation of macrophages. *Journal of Proteomics*. 2012;75(18):5523-5532.
68. Demeure K, Quinton L, Gabelica V, De Pauw E. Rational selection of the optimum MALDI matrix for top-down proteomics by in-source decay. *Anal Chem*. 2007;79(22):8678-8685.

69. Debois D, Bertrand V, Quinton L, De Pauw-Gillet M, De Pauw E. MALDI-in source decay applied to mass spectrometry imaging: A new tool for protein identification. *Anal Chem.* 2010;82(10):4036-4045.
70. Calligaris D, Longuespee R, Debois D, et al. Selected protein monitoring in histological sections by targeted MALDI-FTICR in-source decay imaging. *Anal Chem.* 2013;85(4):2117-2126.
71. Resemann A, Paape R, Suckau D. Precise MW determination of intact proteins by multiple charge state analysis of MALDI generated ions. . 2012;Application Note # MT-112.
72. Karas M, Bachmann D, Bahr U, Hillenkamp F. Matrix-assisted ultraviolet laser desorption of non-volatile compounds. *Int J Mass Spectrom Ion Processes.* 1987;78(0):53-68.
73. Vorm O, Roepstorff P, Mann M. Improved resolution and very high sensitivity in MALDI TOF of matrix surfaces made by fast evaporation. *Anal Chem.* 1994;66(19):3281-3287.
74. Helmke RJ, Boyd RL, German VF, Mangos JA. From growth factor dependence to growth factor responsiveness: The genesis of an alveolar macrophage cell line. *In Vitro Cell Dev Biol.* 1987;23(8):567-574.
75. ATCC. NR8383 [AgC11x3A, NR8383.1] (ATCC<SUP>®</SUP> CRL-2192<SUP>™</SUP>). <http://www.atcc.org/products/all/CRL-2192.aspx#culturemethod>. Accessed August, 2nd, 2014.
76. Tennant JR. Evaluation of the trypan blue technique for determination of cell viability. *Transplantation.* 1964;2(6):685-694.
77. Crawford RM, Finbloom DS, Ohara J, Paul WE, Meltzer MS. B cell stimulatory factor-1 (interleukin 4) activates macrophages for increased tumoricidal activity and expression of ia antigens. *J Immunol.* 1987;139(1):135-141.
78. Carswell EA, Old LJ, Kassel RL, Green S, Fiore N, Williamson B. An endotoxin-induced serum factor that causes necrosis of tumors. *Proc Natl Acad Sci U S A.* 1975;72(9):3666-3670.
79. Kannan L, Rath NC, Liyanage R, Lay Jr JO. Effect of toll-like receptor activation on thymosin beta-4 production by chicken macrophages. *Mol Cell Biochem.* 2010;344(1-2):55-63.
80. Next Advance. Protocol for mammalian cell culture homogenization in the bullet blender®. [http://www.nextadvance.com/public/file/protocols/Bullet\\_Blender\\_Homogenizer\\_Protocol\\_Homogenization\\_Mammalian\\_Cell\\_Culture.pdf](http://www.nextadvance.com/public/file/protocols/Bullet_Blender_Homogenizer_Protocol_Homogenization_Mammalian_Cell_Culture.pdf). Updated 2011. Accessed 08/14, 2014.
81. Rudolph C, Adam G, Simm A. Determination of copy number of c-myc protein per cell by quantitative western blotting. *Anal Biochem.* 1999;269(1):66-71.

82. Tansey W. Ultimate freeze-thaw lysis for mammalian cells. [http://www.tanseylab.com/Tansey\\_Laboratory/Protocols\\_files/Ultime%20Freeze%3A%20Thaw%20Olysis.pdf](http://www.tanseylab.com/Tansey_Laboratory/Protocols_files/Ultime%20Freeze%3A%20Thaw%20Olysis.pdf). Updated 2002. Accessed 08/14, 2014.
83. Yao J, Scott JR, Young MK, Wilkins CL. Importance of matrix: Analyte ratio for buffer tolerance using 2, 5-dihydroxybenzoic acid as a matrix in matrix-assisted laser desorption/ionization-fourier transform mass spectrometry and matrix-assisted laser desorption/ionization-time of flight. *J Am Soc Mass Spectrom*. 1998;9(8):805-813.
84. Karas M, Glückmann M, Schäfer J. Ionization in matrix-assisted laser desorption/ionization: Singly charged molecular ions are the lucky survivors. *J Mass Spectrom*. 2000;35(1):1-12.
85. Blatherwick EQ, Van Berkel GJ, Pickup K, et al. Utility of spatially-resolved atmospheric pressure surface sampling and ionization techniques as alternatives to mass spectrometric imaging (MSI) in drug metabolism. *Xenobiotica*. 2011;41(8):720-734.
86. Eikel D, Vavrek M, Smith S, et al. Liquid extraction surface analysis mass spectrometry (LESA-MS) as a novel profiling tool for drug distribution and metabolism analysis: The terfenadine example. *Rapid Commun Mass Spectrom*. 2011;25(23):3587-3596.
87. Parson WB, Koeniger SL, Johnson RW, et al. Analysis of chloroquine and metabolites directly from whole-body animal tissue sections by liquid extraction surface analysis (LESA) and tandem mass spectrometry. *J Mass Spectrom*. 2012;47(11):1420-1428.
88. McEwen AB, Henson CM, Wood SG. Quantitative whole-body autoradiography, LC-MS/MS and MALDI for drug-distribution studies in biological samples: The ultimate matrix trilogy. *Bioanalysis*. 2014;6(3):377-391.
89. Kertesz V, Van Berkel GJ. Automated liquid microjunction surface sampling-HPLC-MS/MS analysis of drugs and metabolites in whole-body thin tissue sections. *Bioanalysis*. 2013;5(7):819-826.
90. Kertesz V, Van Berkel GJ. Sampling reliability, spatial resolution, spatial precision, and extraction efficiency in droplet-based liquid microjunction surface sampling. *Rapid Commun Mass Spectrom*. 2014;28(13):1553-1560.
91. Xindu G, Regnier FE. Retention model for proteins in reversed-phase liquid chromatography. *J Chromatogr A*. 1984;296:15-30.
92. Carr D, ed. *The handbook of analysis and purification of peptides and proteins by reversed-phase HPLC*. 3rd ed. GraceVydac; 2002.
93. Sigma-Aldrich. Discovery BIO wide pore C18. <http://www.sigmaaldrich.com/analytical-chromatography/hplc/columns/discovery-hplc/bio-wide-pore-c18.html>. Accessed 11/11, 2014.

94. Callister SJ, Barry RC, Adkins JN, et al. Normalization approaches for removing systematic biases associated with mass spectrometry and label-free proteomics. *J Proteome Res.* 2006;5(2):277-286.
95. Woo E. In-solution digestion protocol. . Accessed 10/27, 2014.
96. Proteomics & Mass Spectrometry Center. ZipTip sample clean-up. <http://www.danforthcenter.org/docs/default-source/CoreFacilities/ziptip-protocol.pdf?sfvrsn=0>. Accessed 10/27, 2014.
97. Olsen JV, Ong SE, Mann M. Trypsin cleaves exclusively C-terminal to arginine and lysine residues. *Mol Cell Proteomics.* 2004;3(6):608-614.
98. Cottrell JS, London U. Probability-based protein identification by searching sequence databases using mass spectrometry data. *Electrophoresis.* 1999;20(18):3551-3567.
99. UniProt Consortium. Activities at the universal protein resource (UniProt). *Nucleic Acids Res.* 2014;42(Database issue):D191-8.
100. Spengler B. Post-source decay analysis in matrix-assisted laser desorption/ionization mass spectrometry of biomolecules. *J Mass Spectrom.* 1997;32(10):1019-1036.
101. Johnson RS, Martin SA, Biemann K. Collision-induced fragmentation of (M + H)<sup>+</sup> ions of peptides. side chain specific sequence ions. *Int J Mass Spectrom Ion Processes.* 1988;86:137-154.
102. Roepstorff P, Fohlman J. Letter to the editors. *Biol Mass Spectrom.* 1984;11(11):601-601.
103. Gerhard DS, Wagner L, Feingold EA, et al. The status, quality, and expansion of the NIH full-length cDNA project: The mammalian gene collection (MGC). *Genome Res.* 2004;14(10B):2121-2127.
104. Dabiri GA, Young CL, Rosenbloom J, Southwick FS. Molecular cloning of human macrophage capping protein cDNA. A unique member of the gelsolin/villin family expressed primarily in macrophages. *J Biol Chem.* 1992;267(23):16545-16552.
105. Bączek T. Fractionation of peptides in proteomics with the use of pI-based approach and ZipTip pipette tips. *J Pharm Biomed Anal.* 2004;34(5):851-860.